Chapter 5

Antitumor properties, DNA interaction and ligand substitutions

5.1 Introduction

The complexes in this study were designed to exhibit antitumor activity and therefore it was important to test the complexes *in vitro* and study the structure activity relationships. It was apparent that the new titanocene derivatives should display antitumor activities as they were derived from titanocene dichloride for which the antitumor activities have been established. The candidates were selected based on their stability and composition. Two cell lines were selected for the *in vitro* tests. They are HeLa cells, a human cervix epithelioid carcinoma, and CoLo cells, a colorectal carcinoma. Titanocene dichloride was very successful in inhibiting colorectal carcinomas. One use of the test results will be for screening purposes and another to optimize the composition of the complexes. With this information available, by refining the structural features and studying their mode of antitumor action, new improved drugs could be designed. The results will also be discussed with respect to the structural features of the complexes and evaluated against the proposed mechanism of action and possible interaction with DNA.

In the design of the complexes the assumption was made that DNA will be targeted. This assumption is not necessarily correct. Covalent bond formation of the complexes should occur, after displacement of a labile ligand from the coordination sphere of titanium, at oxygen of the phosphate backbone of DNA. Titanium(IV) represents a hard metal center and oxygen is the hardest of the available heteroatoms with bonding properties in DNA. The introduction of condensed heteroaromatic rings in one of the ligands of titanocene derivatives could lead to intercalation or π-stacking into grooves formed by the double stranded DNA helix. For the latter, the number of rings, the size of the plane of the condensed rings and their orientation will be important. It is assumed that if both modes of action could be incorporated in one carefully designed compound their combined effects should

greatly enhanced the antitumor properties of the compound. Recently, Osella and co-workers[1] proposed that the mechanism of antitumor action for ferrocenyl compounds involves an electron transfer process by redox active enzymes in particular body compartments. The ferricinium species interact with water and oxygen to generate a hydroxyl radical ($OH^{\bullet}$) which cleaves the DNA strands and results in cell death. A similar mechanism could also apply for the titanium(IV) species.

5.2 Antitumor activity

Comparison of the test results of the complexes will give some insight of geometric and electronic factors required to improve their antitumor activity. The first set of tests was devised to screen complexes and thereafter the best candidates were selected and compared against the assumptions made with regard to DNA interactions. Titanocene dichloride **(S-01)** was selected as a primary standard and included in a group of compounds for which both CoLo and HeLa cell lines were cultivated to test their antitumor activities. The free ligands dibenzothiophene **(L2-01)**, dibenzodioxin **(L2-03)** and dibenzodioxinthiol **(L3-03)** as well as the complexes **2-05**, **2-08**, **3-05**, **3-09** and **3-10** were selected for testing. The complexes **3-05** and **3-09** have oxygen and sulfur heteroatoms in the rings, respectively and both are thiolato ligands. Complex **2-05** has oxygen atoms in the ring and a direct bond between the metal and a carbon atom of the ring. The antitumor results are shown in Figure 5.1.

In the presentations, 100% growth was taken as the concentration of untreated cells after three days (duration of experiment) and should be seen relative to the number of cells at the start of the experiment (day 0), which was about 43%. A line indicated the data at day 0 is given in the graphs. The results of the complexes that represent a decrease in cell growth compared to day 0, was ignored and not indicated on the graphs. These compounds were taken as not inhibiting cell growth, but to be toxic at these concentrations.

1. D. Osella, M. Ferrali, P. Zanello, F. Laschi, M. Fontani, C. Nervi , G. Cavigiolio, *Inorg. Chim. Acta*, **2000**, *306*, 42.

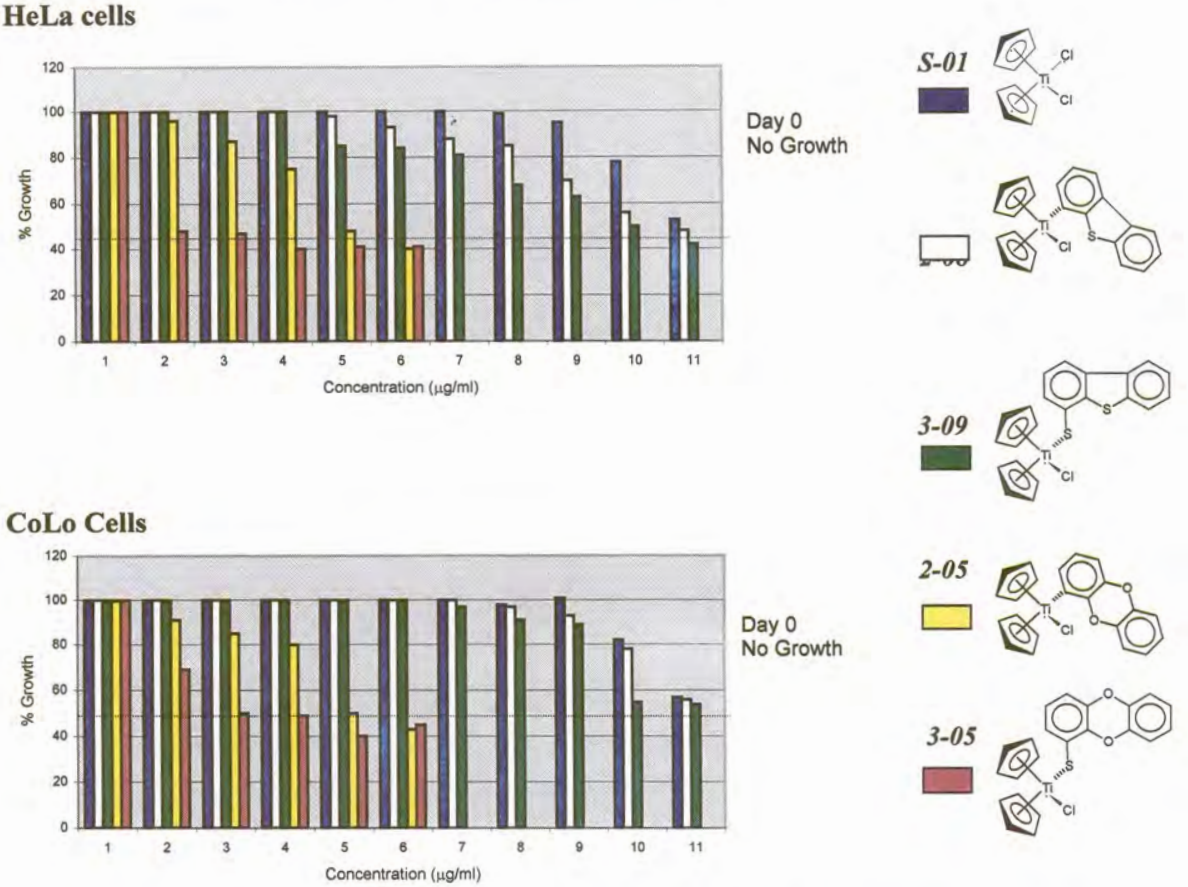

Figure 5.1. Inhibition of HeLa and CoLo cell growth by **S-01**, **2-05**, **2-08**, **3-05** and **3-09**.

It is clear that all the complexes exhibited a concentration dependent suppression of cell growth towards HeLa and CoLo cells. They only differ in the tempo of inhibiting cell growth. The introduction of a heteroaromatic condensed ring ligand improved the activity significantly compared to that of the standard **S-01** and it was further noted that by incorporating the harder oxygen atoms in the rings, cell growth was greatly inhibited. Also the insertion of a spacer atom between the metal and the rings produced improved suppression of cell growth. The free ligands **L2-01**, **L2-03** and **L3-03** were not very active inhibiting cell growth; even at maximum concentrations used, and to simplify the graphs their data are not included. The bis-substituted titanocene dichloride complex, the bisthiolato derivative, **3-10** showed very little activity and was also not included in the graph.

From Figure 5.1 it was clear that the results for the CoLo and HeLa cell lines are very similar and it was decided to continue the rest of the tests only on CoLo cell lines. All growth data of the complexes were compared with the data of the standard **S-01** and the complex that displayed the greatest cell growth inhibition was **3-05**. Due to the large amount of data it was not wise to try and show all the

results on one graph. Instead the data was grouped together according to the objectives of the study mentioned in Chapter 1, and will be discussed accordingly.

Cell growth inhibition results of the model complexes and free ligands

Figure 5.2 displays the test results for the suppression of cell growth of the standards from Figure 5.1, **S-01** and **3-05**, the ligands dibenzofuran **(L2-06)** and dibenzofuranthiol **(L3-06)** and the complexes **2-01** and **3-01**.

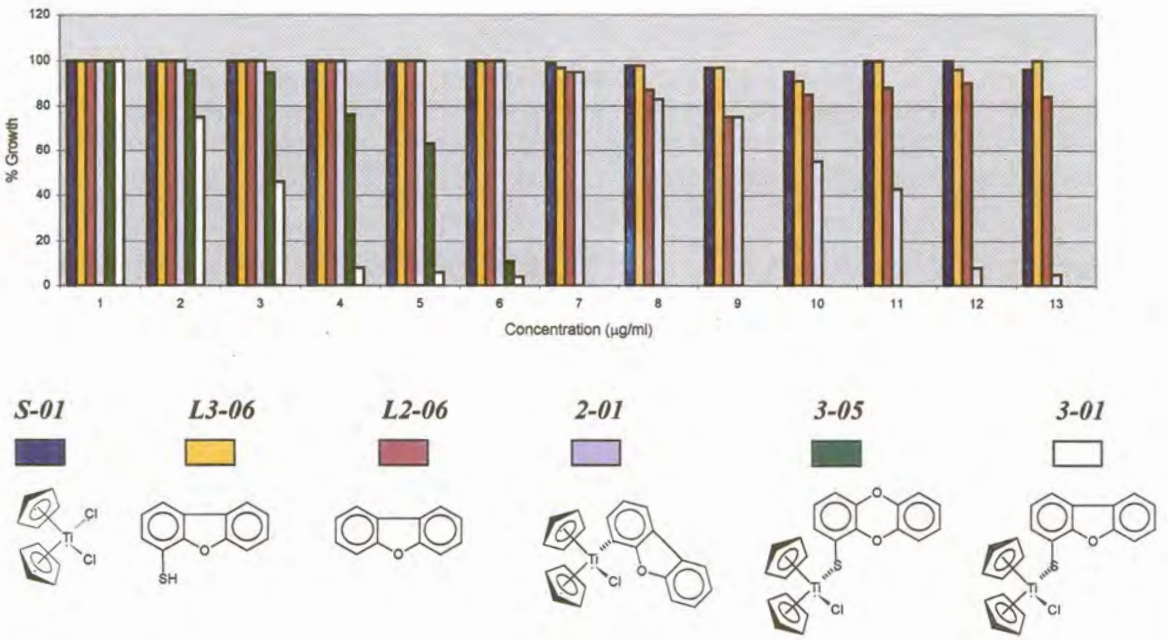

Figure 5.2. Inhibition of CoLo cell growth by **S-01**, **L2-06**, **L3-06**, **2-01**, **3-01** and **3-05**.

The uncoordinated heteroaromatic substrates exhibited very little antitumor effects in this concentration range and it was assumed that the liberation of the ligands played an insignificant role in contributing to the overall antitumor activity. The large inhibition of cell growth by **3-01** and **3-05** is demonstrated in the concentration range 2-7 µg Ti per ml solution. Complex **3-01** tested better than complex **3-05** especially in the 3-5 µg Ti per ml solution region.

(i) The role of the number of condensed rings in the ligand

In Figure 5.3 the cell growth suppression of **S-01** and **3-05** and the thiolato complexes **3-01**, **3-07**, **3-09** and **3-13** are represented against increasing concentrations of the compounds. In all cases inhibition of cell growth were always better by three rings than for two rings in the heteroaromatic ring ligand. This is demonstrated by comparing the test data of the thiolato complexes of benzothiophene (**3-13**) with that of the dibenzothiophene analogue (**3-09**). The former displays only

75% suppression at 14 μg Ti per ml solution compared to complete inhibition of cell growth at this concentration by **3-09**. Complexes **3-01** and **3-05** show complete inhibition of cell growth at a concentration level of 6-7 μg Ti per ml solution, whereas this level of suppression by **3-09** is only reached at 14 μg Ti per ml solution. Complete suppression of cell growth by titanocene dichloride (**S-01**) is only achieved at 460 μg Ti per ml solution which relate to **3-01** being twice as potent as **3-09** which in turn is 33 times more effective than **S-01**.

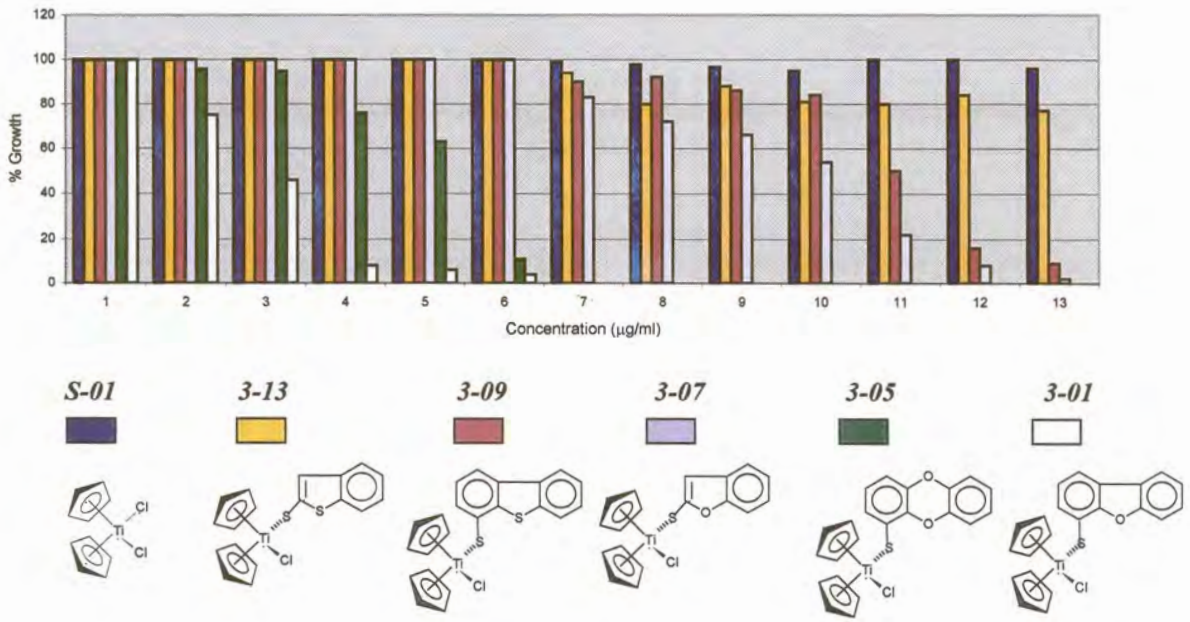

Figure 5.3. Inhibition of CoLo cells by **S-01**, **3-01**, **3-05**, **3-07**, **3-09** and **3-13**.

(ii) The role of the heteroatom(s) in the condensed rings of the ligand

In Figures 5.3 and 5.4 the role of different heteroatoms in the rings of the condensed heteroaromatic ligand is also demonstrated. It is clear that the ligands with oxygen as heteroatom achieved better inhibition results than their sulfur analogues.

(iii) The number of heteroatoms in the ligand

In Figure 5.4 the cell inhibition data of the two standards, **S-01** and **3-05** and the complexes **2-01**, **2-05** and **3-01** are given. It follows that the complexes with one oxygen heteroatom in the condensed ring was more effective in suppressing cell growth than the complexes with two oxygen atoms.

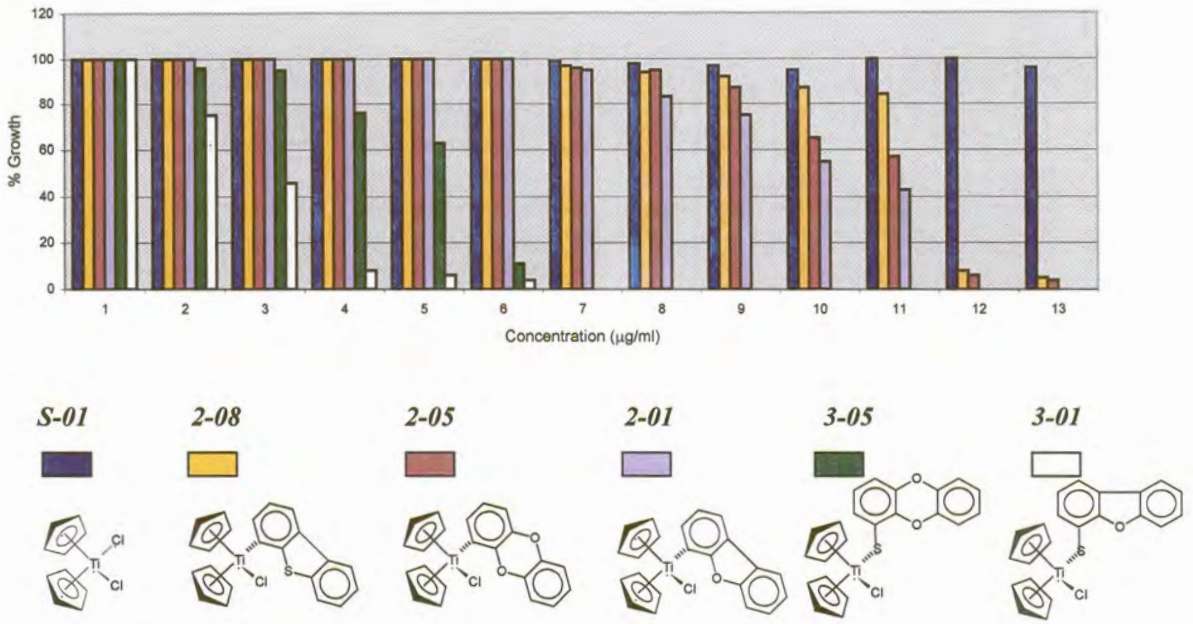

Figure 5.4. Inhibition of CoLo cells by **S-01**, **2-01**, **2-05**, **2-08**, **3-01** and **3-05**.

(iv) The role of substituents on the ring ligand

Figure 5.5 shows the results of the two standards, **S-01** and **3-05** and the complexes **2-01**, **2-03**, **3-01** and **3-03**. The substituent on the heteroaromatic ring ligand does not seem to have much of an effect on antitumor activity of the complex. This is evident in comparing **2-01** with **2-03** or **3-05** with **3-03.** It was expected that a methyl group on the ring ligand would have an effect on intercalation.

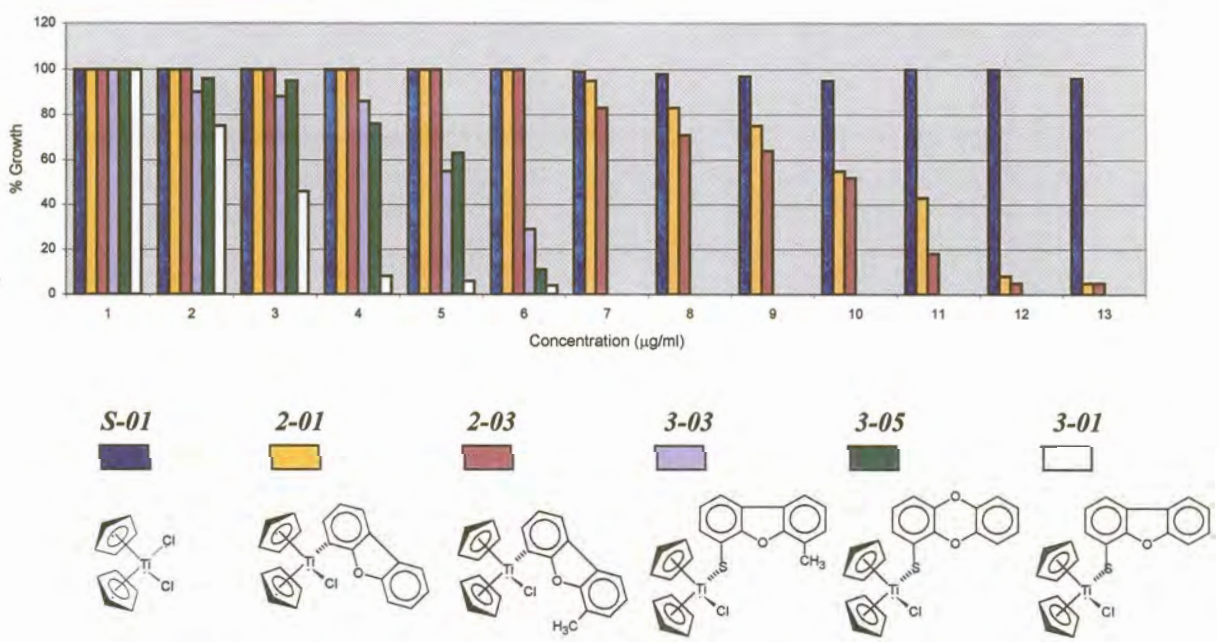

Figure 5.5. Inhibition of CoLo cells by **S-01**, **2-01**, **2-03**, **3-01**, **3-03** and **3-05**.

(v) The role of a spacer inserted between the metal and the rings

Figures 5.4 and 5.5 verify the observation made from Figure 5.1 that the insertion of a spacer atom between the metal and the heteroaromatic rings improve suppression of cell growth.

(vi) The role of the non-cyclopentadienyl ligands

In Figure 5.6 the results of the suppression of cell growth of the two standards, **S-01** and **3-05** and the complexes **3-01**, **3-02**, **3-06** and **2-11** are given. The complexes with one chloro ligand replaced by a thiolato ligand tested much better than the complexes where none or both chloro ligands were replaced by thiolato ligands. Thus, the order of activity of inhibiting cell growth is $[TiCp_2Cl_2]$ < $[TiCp_2(SR)_2]$ < $[TiCp_2(SR)Cl]$. Also the complex with a bidentate metallacyclic ring ligand had less activity than the complexes with one thiolato ligand.

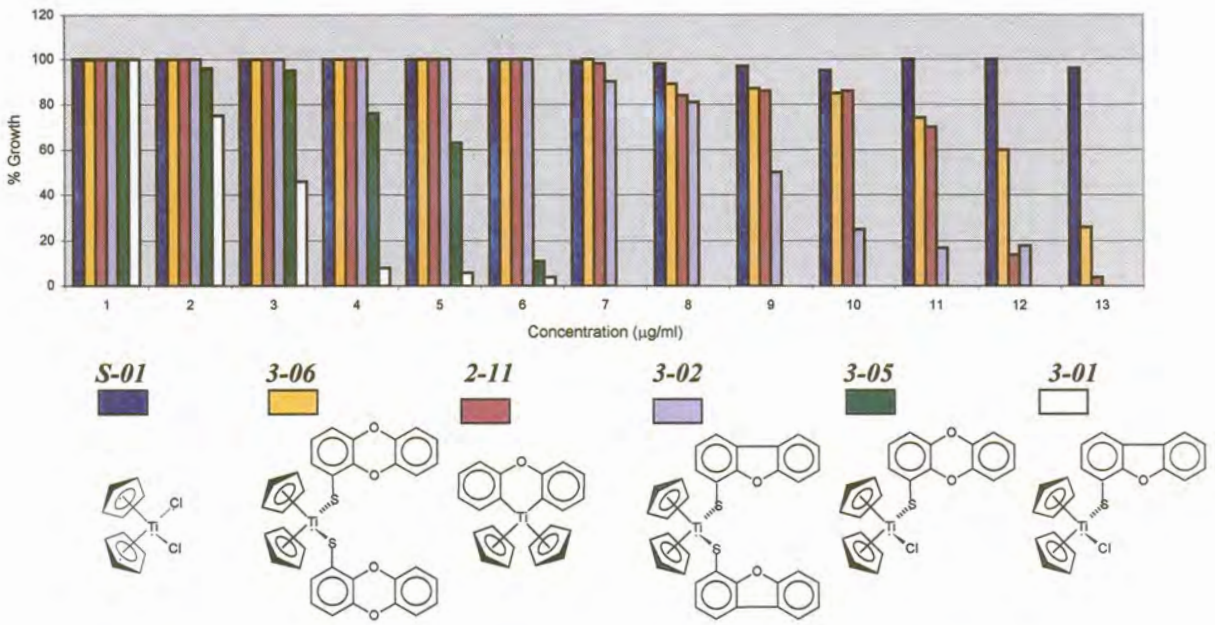

Figure 5.6. Inhibition of CoLo cells by **S-01**, **2-11**, **3-01**, **3-02**, **3-05** and **3-06**.

5.2.1 Conclusions

Of all the complexes tested for inhibiting cell growth, complex **3-01** gave the best results. This compound meets all the requirements of design implicated by the assumptions made for interacting with DNA. It has (i) a labile chloro ligand to afford a vacant coordination site for covalent bonding and (ii) display a condensed heteroaromatic ligand of favorable size for intercalation. The question remains whether the orientation of the different ligands in the complexes are such that they could participate in the above interactions effectively.

5.3 Structural features vs. antitumor activities

Correlation of activity with structure were studied by determining the solid state structures of **2-02**, **2-05**, **2-08** and **3-09** and comparing the structural features with cell growth suppression data. The structural requirements for effective covalent bond formation as well as intercalation into the major groove of DNA were compared with the molecular geometries of the complexes. The relative orientations of the two non-cyclopentadienyl ligands with respect to the two cyclopentadienyl ligands are important.

Figure 5.7 shows the structures of **2-05** and **2-08** that display the condensed ring ligand bound directly to the metal fragment. The metal, chloro and condensed heteroaromatic ring ligand are all part of the plane and these complexes are examples of metallointercalators. Hence only one of the modes of interaction, i.e. either covalent bonding or intercalation could be possible. The structures clearly show that this geometry would not be ideal for covalent bonding as well as intercalation into the major groove.

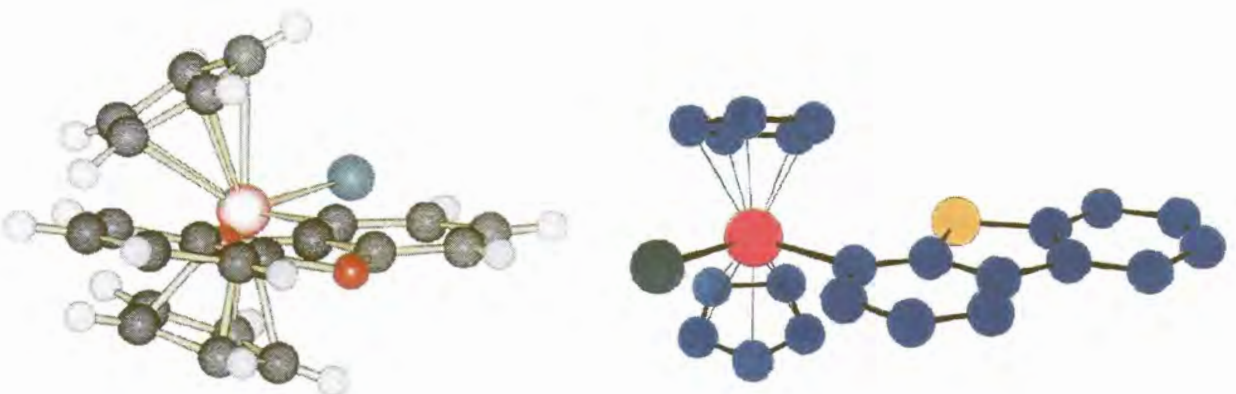

Figure 5.7. Molecular structures of **2-05** and **2-08**.

Figure 5.8 represents the molecular structure of a thiolato complex **3-09** with a sulfur atom as a spacer atom between the metal and the rings. This geometry is better suited for both intercalation and covalent bond formation, because the ligand is more flexible.

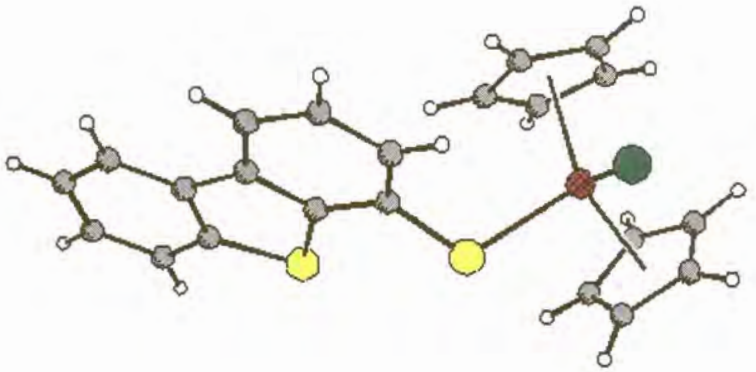

Figure 5.8. Molecular structure of **3-09**.

Figure 5.9 shows the complex with two heteroaromatic ring ligands. This complex lacks an easily replaceable chloro ligand for covalent bond formation with DNA. Furthermore, the two rings are not configured ideally for intercalation.

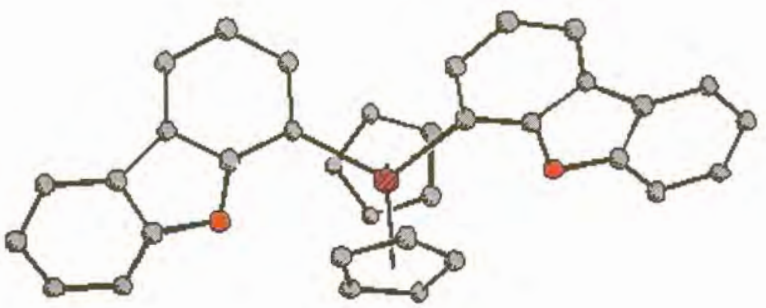

Figure 5.9. Molecular structure of **2-02**.

A mechanism, based on the assumptions that the metal will covalently bond to an oxygen of the phosphate backbone of DNA and in addition be able to intercalate into the major groove of DNA, was tested by modeling the orientation of three rings bonded (i) directly and (ii) via a spacer atom to the metal within a fragment of DNA. In the first diagram (Figure 5.10) on the left side, the complex is shown being bonded covalently to the DNA backbone, but due to the geometry is not able to intercalate effectively. In the second diagram the complex is shown with a spacer atom between the metal and the intercalating rings. This allows for far greater flexibility making intercalation and simultaneous covalent bonding a reasonable assumption.

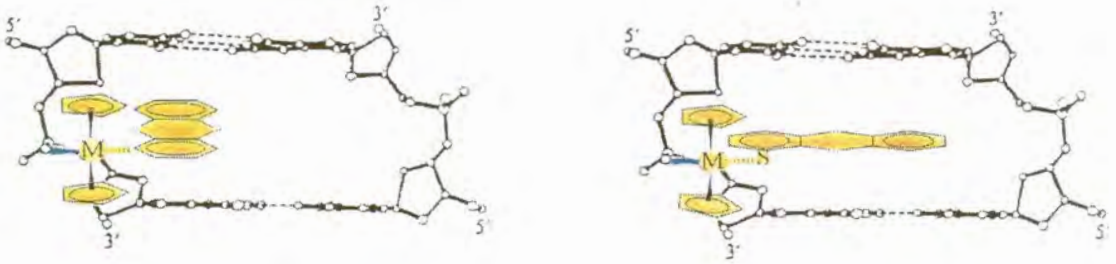

Figure 5.10. Geometrical constraints of complexes interacting with a double stranded DNA fragment.

5.3.1 Conclusions

Good correlation was found between antitumor activity and the geometrical features of the compounds according to the requirements of the assumptions for both covalent bond formation and intercalation. The complex **3-09,** that are structurally best suited to participate in both modes of interaction with DNA of the compounds studied structurally, tested the best in inhibiting cell growth.

5.4 Ligand substitution in aqueous medium

To study the replacement of the ligands in the thiolato complexes, titanocene dichoride **S-01** was compared to **3-01** (the complex that showed the greatest cell growth inhibition) and the bisthiolato complex **3-02**. A 0.25M solution of each complex in d^6-DMSO was diluted in a saline (D_2O) solution in a 3:1 ratio. The solutions were kept at 37°C. The reaction was followed spectroscopically with ^1H NMR and the chemical shifts recorded in the cyclopentadienyl and heteroaromatic regions as functions of time, as shown in Figures 5.11, 5.12, 5.13 and Appendix **F**. The results of **S-01**, **3-01** and **3-02** are compared.

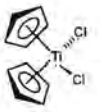

S-01

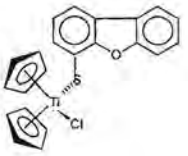

3-01

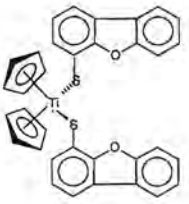

3-02

0h

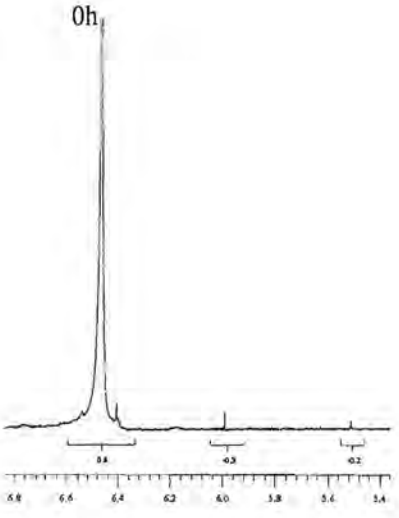

0h

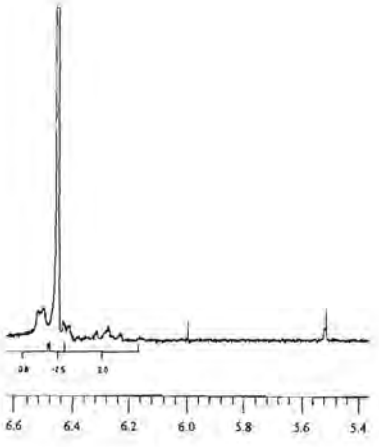

0h

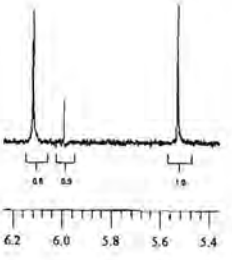

1h

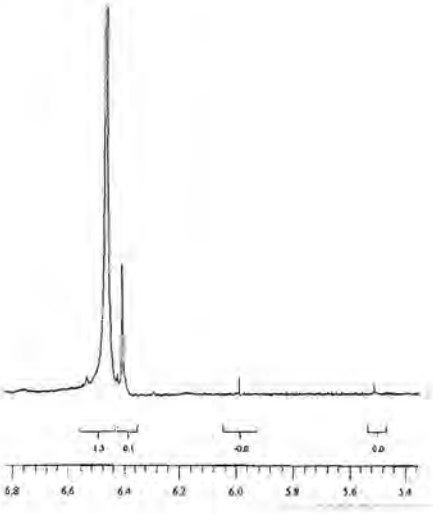

1h

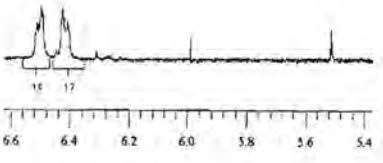

1h

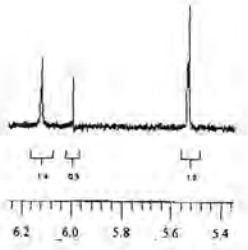

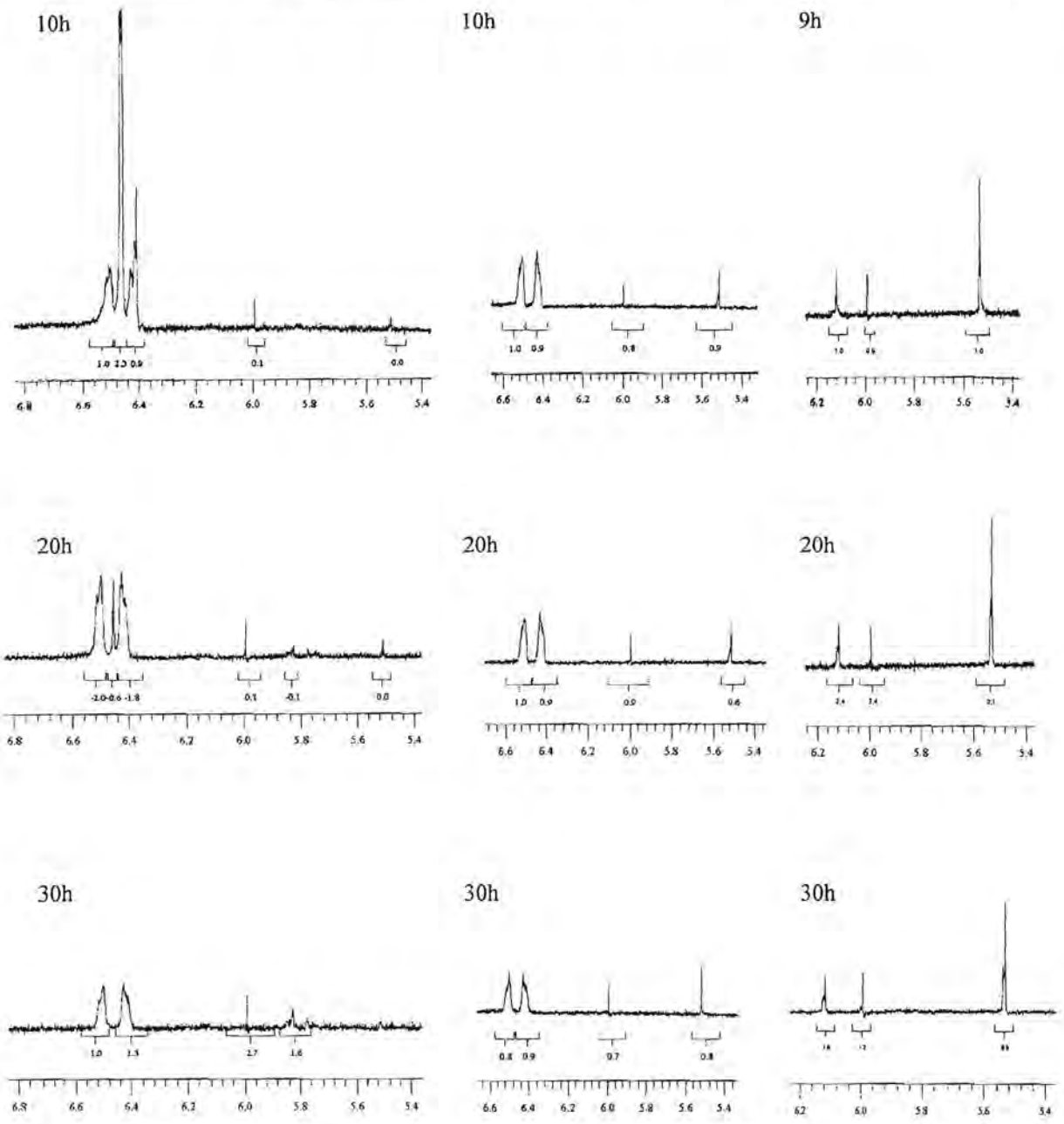

Figure 5.11. Comparison of Cp resonances in the ^{1}H NMR spectra of **S-01**, **3-01** and **3-02**.

The hydrolysis of the Cp rings of **S-01** started after 1h, were only significant after 10h and complete after 30h. For complex **3-01** hydrolysis started immediately and was complete after 1h. In fact, on mixing with the saline mixture the thiolate ligand was quickly replaced by Cl to give titanocene dichloride and dibenzofuranylthiol as products. Hence, after a short period of time the spectra are identical to the final spectrum of **S-01**. The fast disappearance of titanocene dichloride is ascribed to the presence of the thiolato ligand in solution. See Scheme 5.1. In complex **3-02** there was no visible

hydrolysis as compared to **S-01** and **3-01**, and the ratio of the peaks changed very little over time. Although **3-01** converts to **3-02**, the opposite is not true, not even in a saline mixture. From this information it was concluded that the dominant process for **3-01** in saline solution is equilibrated between titanocene dichloride and itself, whereas **3-02** is inert towards substitution reactions.

Displacement kinetics of the thiolato ligands

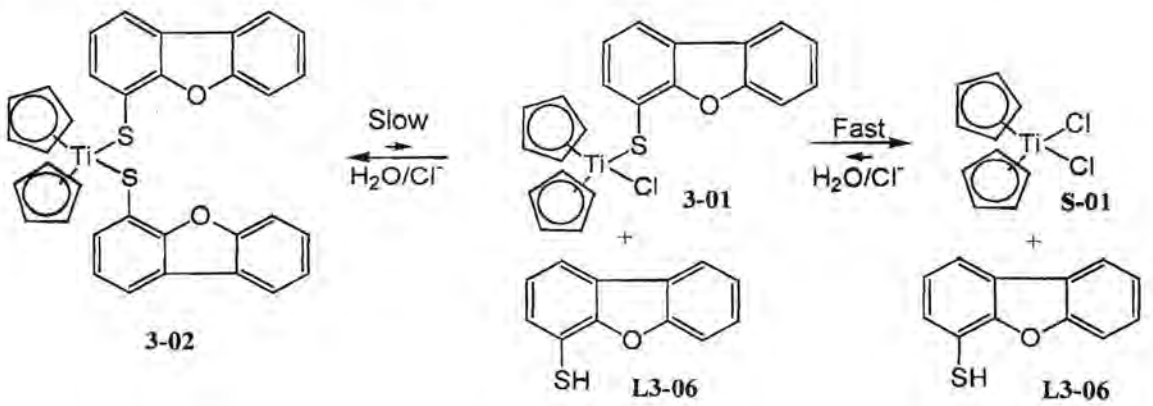

*Cp-Hydrolysis of **S-01** and **3-01***

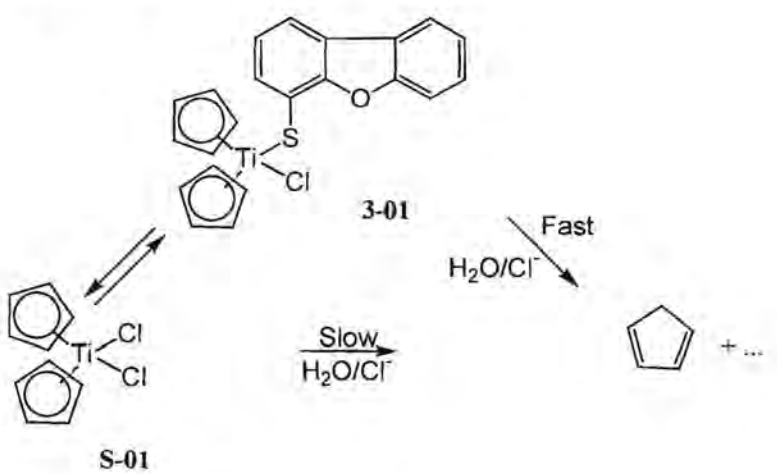

Scheme 5.1

The chemical shifts of the ^{1}H NMR spectra of **3-01** and **3-02** were also studied in the aromatic region to obtain information of the substitution of the thiolato ligands. Figure 5.12 displays the spectra for **3-01** at the start of the experiment and at the end after 30h. The chemical shifts of **3-01** in the aromatic region were assigned to those of dibenzofuranylthiol and did not change at all between the start of the experiment and after 30h. This result supports the hydrolysis data of the cyclopentadienyl rings and confirms rapid displacement of the thiolato ligand.

0h

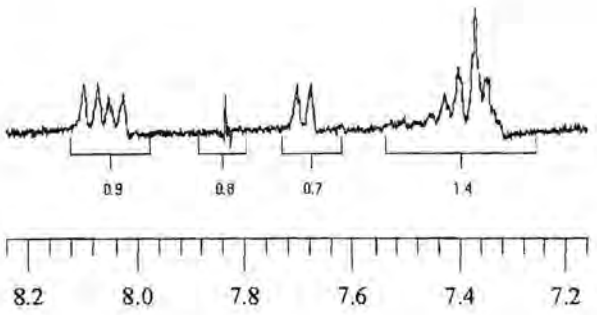

30h

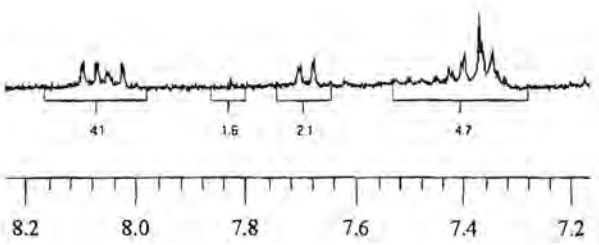

Figure 5.12. ^{1}H NMR resonances in the aromatic region of **3-01**.

By contrast, the resonances assigned to the thiolato ligand of **3-02** changed slowly over time. Figure 5.13 display patterns for the chemical shifts that changes gradually. In the time frame 0-3h, resonances of the bisthiolato complex **3-02** dominates, whereas, a similar pattern is found for **S-01**, i.e. uncoordinated dibenzofuranylthiol, after 30h. In the intermittant time (6-9h) the pattern belongs to a solution containing both **3-02** and the thiol of **3-01**. The inertness of the thiolato ligands in solution of **3-02** and the high rate of displacement of the thiolate ligand of **3-01** is again demonstrated by these results.

0h

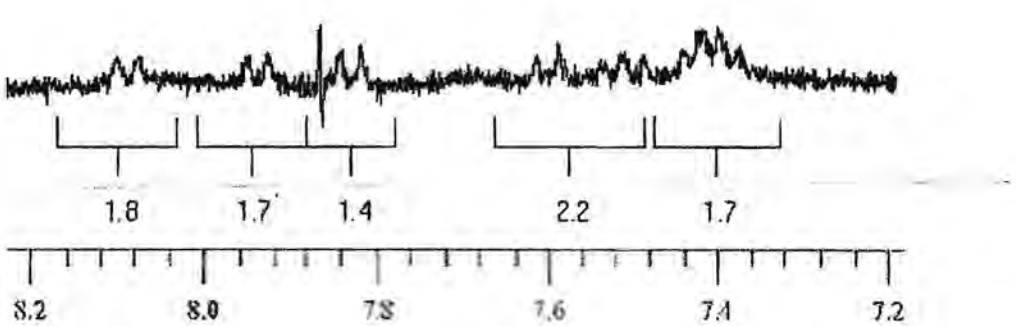

3h

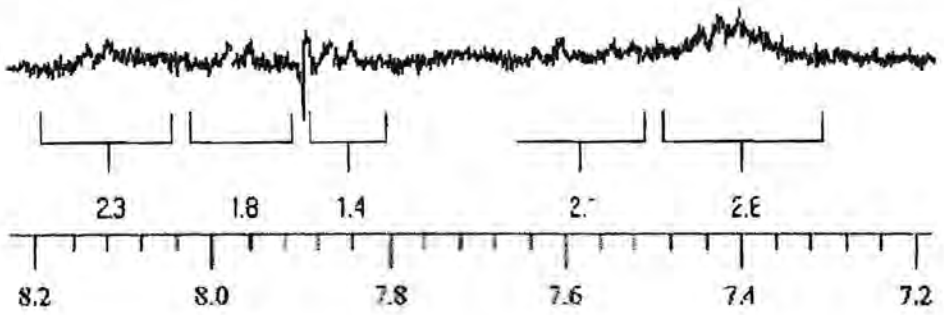

7h

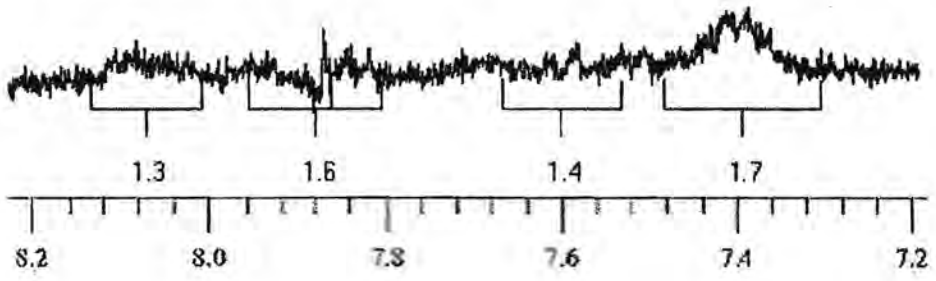

20h

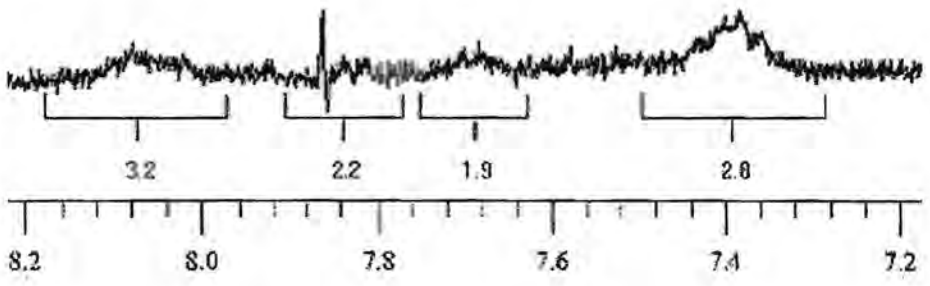

30h

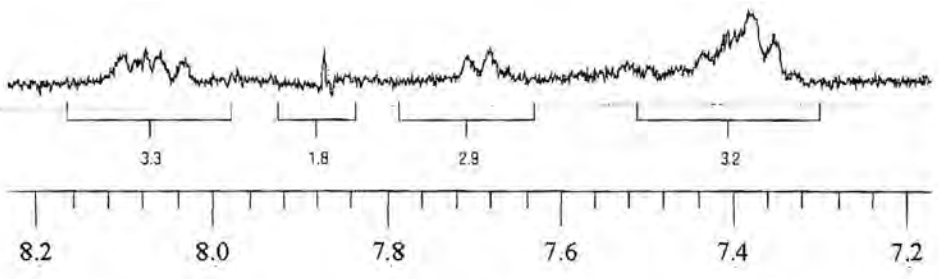

Figure 5.13. Substitution of the thiolato ligand of complex **3-02**.

5.4.1 Conclusions

The data support substitution of ligands in the order SR, Cl > Cp and rates the stability against substitution of the complexes in the order $[TiCp_2(SR)_2]$ > $[TiCp_2Cl_2]$ > $[TiCp_2(SR)Cl]$ under the conditions of a DMSO/saline solution. The kinetic data does not support the initial assumptions pertaining to interactions with DNA. It does however show that **3-01,** which is the strongest inhibiter of cell growth, is also the least stable compound under the conditions applied.

5.5 Intercalation studies

The complexes were designed to intercalate with DNA and it was decided to perform some DNA intercalation tests using a technique based on flow cytometry. This was done to see if there was a correlation between antitumor activity and intercalation. Flow cytometry gives scattering information which could be applied to measure the winding characteristics of nucleoids. This is done by comparing the forward and side scattering of laser light through the substrate under regulated conditions. Figure 5.14 shows a model of the super coiled DNA that was used in the experiments. Intercalation will cause the DNA to unwind and then further intercalation will cause the DNA to wind up in the opposite direction. It is these phases of winding and unwinding that cause the scattering of the laser light to vary. The more complex and compact (dense) the structure of the substrate the greater the side scattering. By comparing the forward and side scattering as a function of concentration it should be possible to determine whether the complex will intercalate or not.

Figure 5.14. The unwinding and winding of super coiled DNA due to intercalation.

The intercalating abilities, as derived from the flow cytometry results of the complexes, were compared against similar data obtained for the known intercalators ethidium bromide (Figure 5.15),

doxorubicin (Figure 5.16) and propidium iodide (Figure 5.17)[2]. At low concentration, where intercalation takes place, the nucleoids are unwound leading to a less dense substrate and an increase in forward scattering (FS) of the laser light and a comparably smaller increase in side scattering (SS). This is seen in the concentration range of 0.2-30.0 μg intercalator/mL. Intercalation will however lead to rewinding of the DNA at higher concentration and the difference between forward scattering and side scattering will decrease again to give a characteristic curve as seen in Figures 5.16 – 5.17. The sharp increase in side scattering at very high concentrations is ascribed to a much denser substrate resulting from an increase in the number of covalent bond formations of the complexes with DNA.

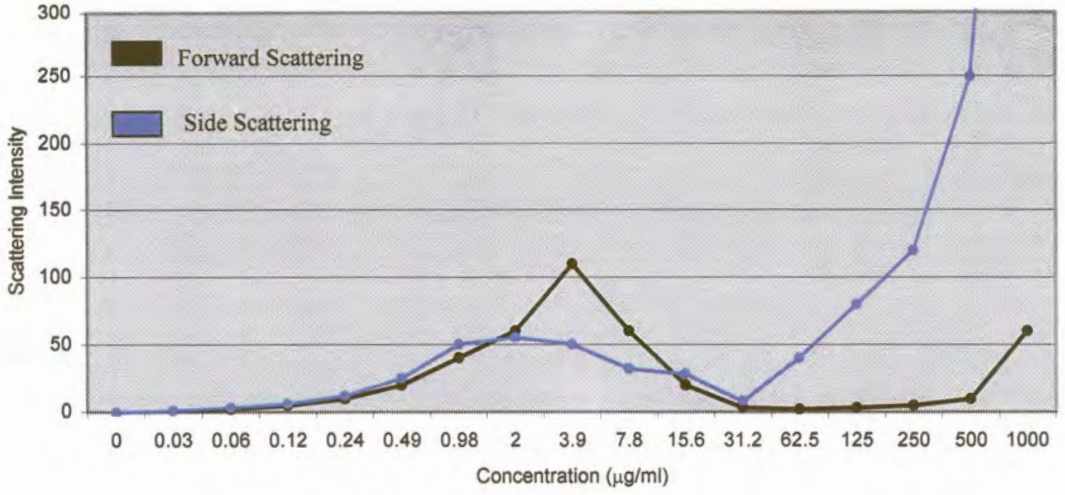

Figure 5.15. Intercalation of ethidium bromide with DNA.

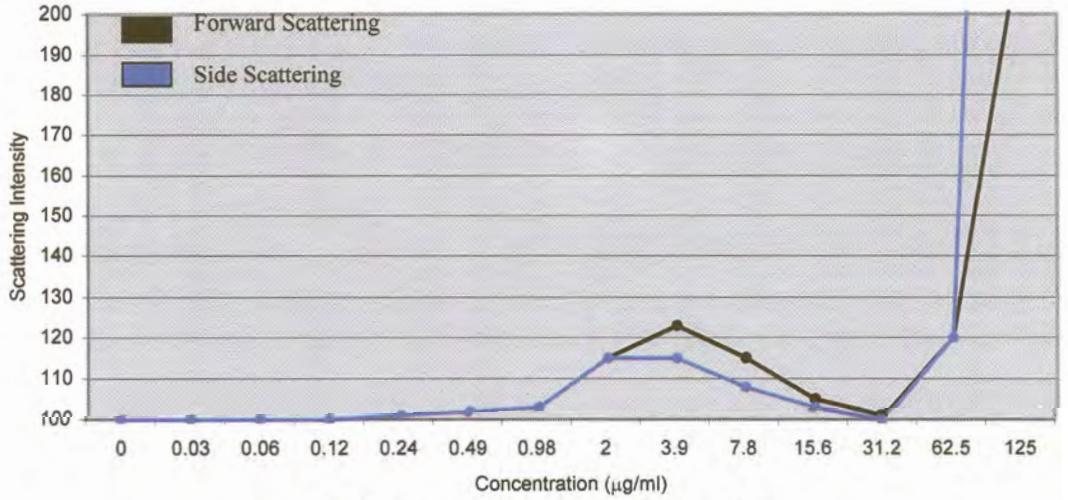

Figure 5.16. Intercalation of doxorubicin with DNA.

2. S. J. Lippard, *Acc. Chem. Res.*, **1978**, *11*, 211.

Figure 5.18 shows that very little unwinding of DNA occurred for **S-01** and therefore did not intercalate as the amount of forward scattering and side scattering are approximately constant at all concentrations. The results are in agreement with what was expected because the titanocene dichloride has no planar heteroaromatic ligands required for intercalation.

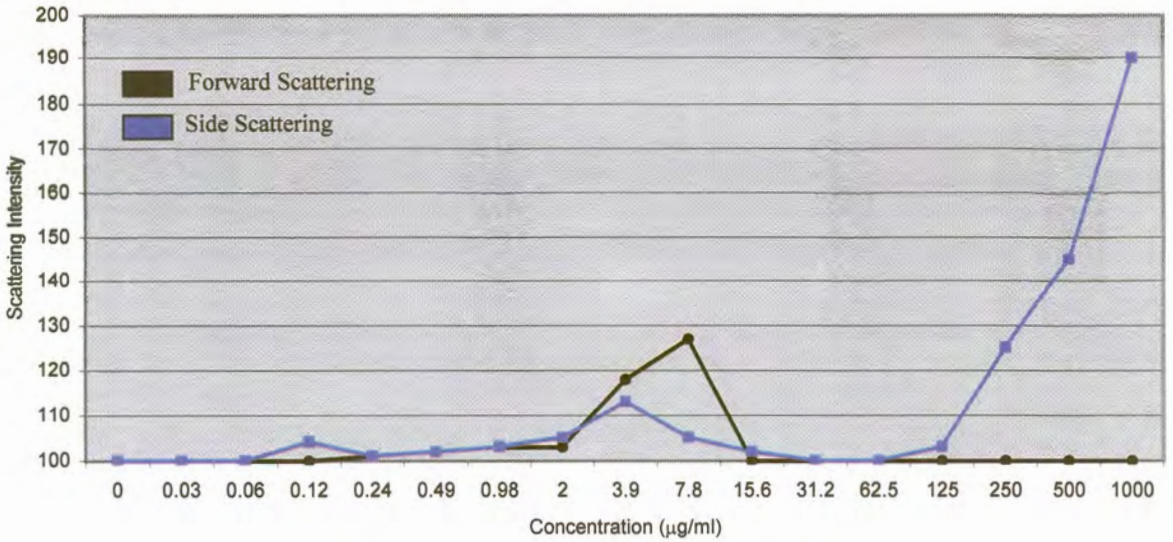

Figure 5.17. Intercalation of propidium iodide with DNA.

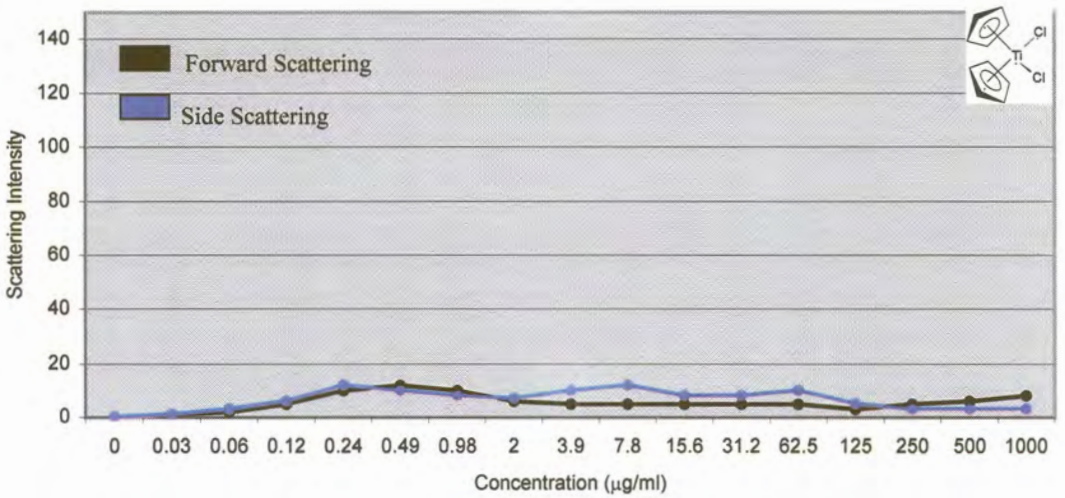

Figure 5.18. Intercalation studies of **S-01** with DNA.

Figure 5.19 shows the profile for **3-01** and it was concluded that no intercalation took place. At 2.4µg/ml the small difference between forward vs. side scattering was considered insignificant. The increase of side scattering is only observed at higher concentrations. This was ascribed to bond formation of **3-01** and an oxygen atom of the phosphate groups of DNA and as a result leading to a denser structure. This could also be interpreted that the mechanism of action of the new complexes is different from that of **S-01**.

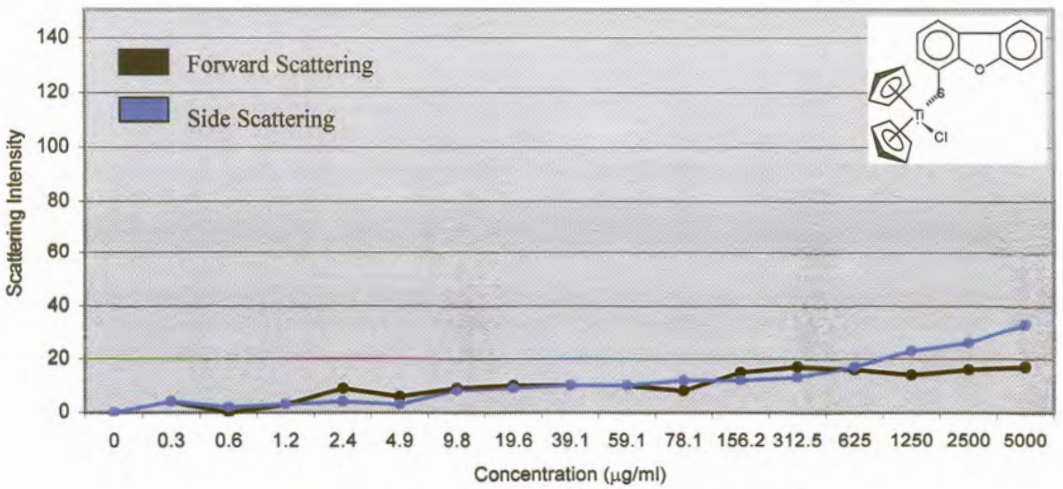

Figure 5.19. Intercalation studies of **3-01** with DNA.

Figure 5.20 shows the graph of one of the uncoordinated heteroaromatic substrates **L2-06** that displayed the same profile typical of that of an intercalator. No further interaction with DNA was observed at high concentrations.

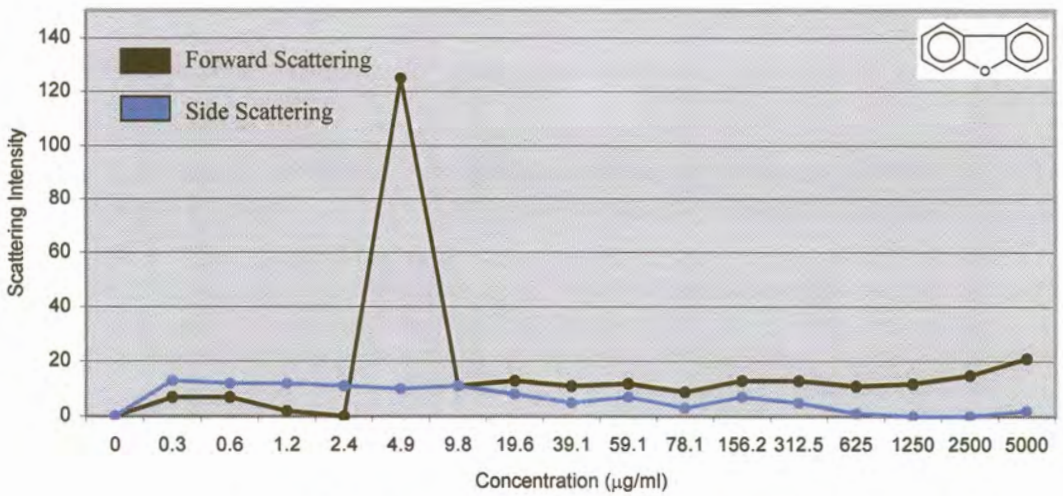

Figure 5.20. Intercalation studies of **L2-06** with DNA.

In Figure 5.21 no intercalation of the complexes with DNA was observed at lower concentrations, but at very high concentrations there was a sudden increase in side scattering. A possible explanation is that the complexes are sticking to the DNA strand and this causes increased scattering of the laser light. As observed in Figure 5.18, complex **S-01** showed no increase in side scattering at high concentrations. The complexes with thiolato ligands (**3-01** and **3-09**) showed significant increase in side scattering at higher concentrations.

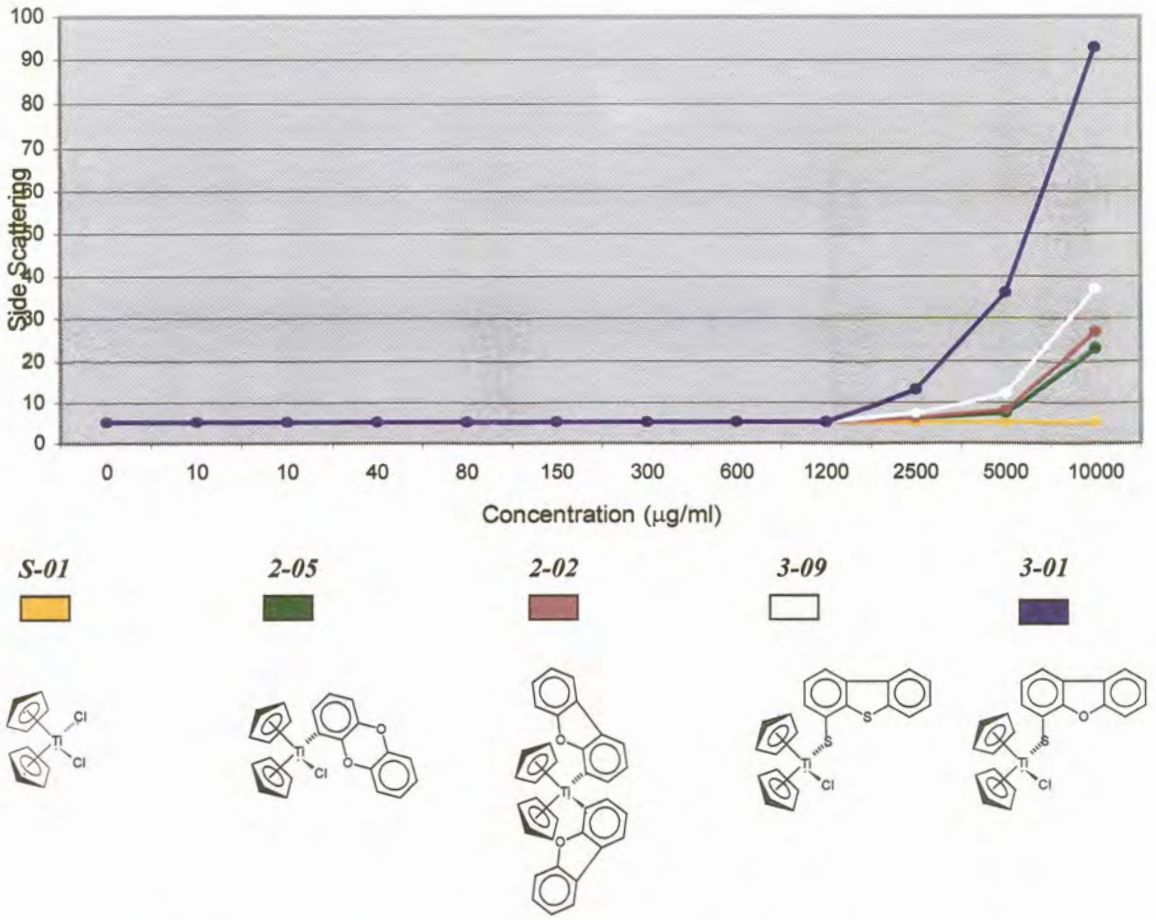

Figure 5.21. DNA bond formation of some complexes based on side scattering data.

5.5.1 Conclusions

The flow cytometry results confirmed that the species did indeed interact with DNA, but not by means of intercalation. When comparing the side scattering of the different compounds (Figure 5.21) the complexes that were expected to intercalate least caused less side scattering. This is not a contradiction but could mean that they have lower activities because their covalent binding ability to DNA was also weaker or slower. The two complexes that performed best in the antitumor tests caused increased side scattering at higher concentrations. It was concluded that the antitumor activity of the new titanocene derivatives with a heteroaromatic ring ligand could be ascribed to covalent bond formation with DNA, but not because of intercalation into the DNA grooves.

5.6 Summary of test results and DNA interaction

From these studies it was concluded that the increased antitumor properties of the titanocene derivatives result from covalent bond formation to DNA, most likely the phosphonate backbone of DNA. This observation is supported by studies of Sadler and co-workers who recently showed that the Ti(IV) hydrated ion would bind preferentially at an oxygen atom of the phosphate backbone of DNA[3]. The cytometry results do not, however, explain the increased activity of the complexes containing heteroaromatic ring ligands compared to titanocene dichloride. The thiolato ligands must play an important role to increase the activities. At first it was thought that the combined effect of titanium ion and the heteroaromatic substrate could account for the higher activities, but it was shown that for most heteroaromatic rings which were tested separately, very little antitumor activity was detected. The complexes with the highest antitumor activities were those that were the least stable in aqueous solution as was shown with the ligand substitution studies. The heteroatom in the mono thiolate complex could facilitate favourable substitution of the remaining chloro ligand in these complexes. This could also account for the fact that oxygen tested better than sulfur, as titanium is a hard metal centre.

At this point of time with the data generated from cell growth inhibition experiments, structural features and compositions of complexes, stability in saline solution against ligand substitution and intercalation studies, other mechanisms of interaction that differ from the pre-proposed modes of interaction with DNA, need to be considered. The inclination is to more seriously investigate the possibility that the antitumor activity of the titanium complexes of this study may arise from the ability of the titanium ion to take part in charge transfer processes as was proposed by Osella[1] for ferrocenyl species. It was not possible to determine the composition of the titanium species that bind to DNA. This implies that titanium is delivered at a rate determined by the thiolato ligands in the cells, leading to the formation of highly active radicals ($OH^{\bullet}$ and $O_2^{\bullet}$) which could cleave DNA strands and cause cell deaths. This could explain the concentration dependence of the antitumor activities of the complexes. However, unlike Fe(II)/Fe(III) the titanium couple Ti(III)/Ti(IV) is unstable in aqueous medium and without further studies the Osella radical mechanism seems a less likely explanation for the titanocene derivatives.

3. M. Quo, Z. Quo, P. J. Sadler, *J. Biol. Inorg. Chem.*, **2001**, *7*, 698.

Chapter 6

Experimental

6.1 General

The following conditions applied throughout the synthesis of new complexes, unless stated otherwise in the method. Standard Schlenk methods were used as described by Shriver[1]. All the solvents were distilled under inert reflux conditions and stored under dry nitrogen gas[2]. THF was used immediately after distillation. Column chromatography was performed by circulation of cooled *iso*-propanol through the column jacket. Products were stored at 5°C under dry argon or nitrogen gas.

Characterization of complexes was done in an inert atmosphere, where possible. Melting points were determined on a Gallenkamp Melting Point Apparatus and are uncorrected. Nuclear magnetic resonance spectra were recorded on a Bruker AC-300 spectrometer. The ^{1}H and ^{13}C NMR spectra were measured at 300.135 and 75.469MHz, respectively. Chemical shifts are reported as δ-values in parts per million (ppm) using the deuterated solvent signal as the internal reference. Deuterated chloroform (calibrated at δH = 7.2400 ppm) was used as the routine solvent to record spectra and where not appropriate, deuterated DMSO (calibrated at δH = 2.4900 ppm) was used. Microanalysis was obtained from the analytical section of the Division for Energy Technology of the Council of Scientific Research (CSIR) in Pretoria. High-resolution mass spectra were recorded on a Finnegan 8200 spectrometer.

Silica gel plates, silica gel 60 (0.200 – 0.063mm) and all other chemicals used are commercially available, except dibenzo[1,4]dioxin, which was synthesized according to methods described in literature[3]. All solid reagents were used without prior purification, while the liquid reagents were distilled. Deprotonations were carried out with *n*-BuLi, which was a 1.6mol/dm^3 solution in hexane.

---

1. D. F. Shriver, M. A. Drezdzon in *The Manipulation of Air-Sensitive Compounds*, 2nd edition, John Wiley and Sons, New York, **1986**.

2. D. D. Perrin, W. L. F. Armarego, D. R. Perrin in *Purification of Laboratory Chemicals*, 2nd edition, Pergamon, New York, **1980**.

3. H. H. Lee, W. A. Denny, *J. Chem. Soc. Perkin Trans. I*, **1990**, 1071-1074.

6.2 Lithiation and synthesis of heteroaromatic compounds

The lithiation procedures of the heteroaromatic molecules are summarized in Table 6.1 and the synthesis of heteroaromatic compounds are found in Table 6.2.

General lithiation methods using n-butyl lithium

Method A: At -30 °C n-butyl lithium (7.0ml, 11mmol) was added to a stirred solution of the heteroarene in 20ml THF. After stirring for the indicated time, the mixture was cooled to -50°C for subsequent reactions.

Method B: At -30 °C TMEDA (3.4ml, 11mmol) was added to a stirred solution of the heteroaromatic substrate in 20ml THF. n-Butyl lithium (7.0ml,11mmol) was added and the solution stirred for the required time at -30 °C. The mixture was cooled to -50°C for subsequent reactions.

Method C: At 0°C 20ml THF was added to a stirred solution of n-butyl lithium (7.0ml, 11 mmol) in 20ml hexane. The solution was cooled to -50°C and the heteroarene added slowly (over 1 minute). After heating to –20 °C, the mixture was stirred for the indicated time and cooled to -50°C for subsequent reactions.

Method D: At room temperature (RT) 150ml hexane, 100ml diethyl ether and the heteroarene was mixed. TMEDA (15.0ml, 20.0mmol) and n-butyl lithium (14.0ml, 20.0mmol) was added subsequently. The solution was allowed to stand for the indicated time period at RT and a precipitate settled out. The suspension was cooled to -50°C for subsequent reactions.

Method E: At -30 °C n-butyl lithium (7.0ml, 11mmol) was added to a stirred solution of the heteroaromatic substrate in 20ml THF. After stirring for the indicated time, the temperature was raised to 0°C and stirring continued for another 2h. The mixture was cooled to -50°C for subsequent reactions.

Method F: At -30 °C n-butyl lithium (7.0ml, 11mmol) was added to a stirred solution of the heteroarene in 20ml THF. The temperature was raised to 0°C and stirred for the required time. The solution was cooled to -50°C for subsequent reactions

Table 6.1 Lithiation procedures of the heteroaromatic substrates used in this study.

Lithiated Precursor	Starting Compound	Method	Amount of starting material (mmol, g)	Reaction time (h)	Colour of lithiated product	Reference
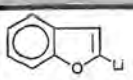	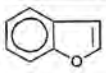 **L2-05**	C	10.0; 1.1ml	30min.	Pink turns yellow	4
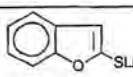	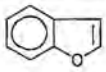 **L2-05**	C + G	10.0; 1.1ml	30min. + 20min.	Bright yellow	4
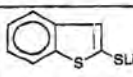	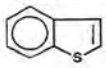 **L2-02**	A + G	10,0; 1.34	30min. + 20 min.	Orange-yellow	4, 5
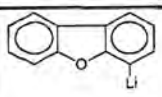	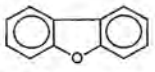 **L2-06**	A	10.0; 1.68	5	Bright yellow	4, 6
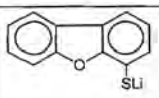	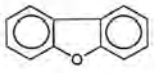 **L2-06**	A + G	10.0; 1.68	5 + 2	Orange	4, 7
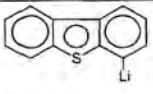	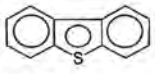 **L2-01**	F	10.0; 1.84	5	Deep orange	4, 7
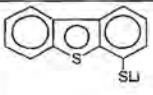	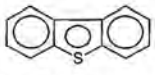 **L2-01**	F + H	10.0; 1.84	5 + 1	Deep orange turns green, then yellow	4, 7
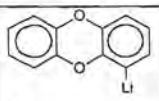	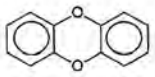 **L2-03**	B	10.0; 1.84	1	Bright yellow	4, 8

4. L. Brandsma, H. Verkruijsse, *Preperative Polar Organometallic Chemistry 1*, Springer-Verlag (Berlin, Heidelberg) **1987**, 215-235

5. H. E. Gschwend, H. R. Rodriguez, *Org, React*, **1979**, *26*, 1.

6. H. Gilman, S. Gray, *J. Org. Chem.*, **1958**, *23*, 1476.

7. C. Cuehm-Caubere, S. Adach-Becker, Y. Fort, P. Caubere, *Tetrahedron*, **1996**, *52*, 9087.

8. B. D. Palmer, M. Boyd, W. A. Denny, *J. Org. Chem.*, **1990**, *55*, 438.

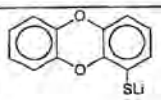 **L2-03**	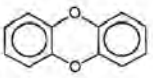	B + G	10.0; 1.84	1 + 15min.	Orange-brown	4, 8
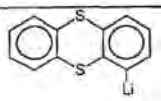 **L2-04**	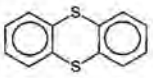	B	10.0; 2.16	2	Bright yellow	4, 10
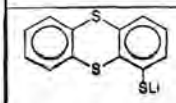 **L2-04**	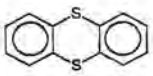	B + G	10.0; 2.16	2 + 15min.	Orange-brown	4, 10
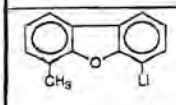 **L2-07**	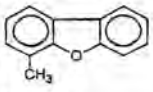	E	10.0; 1.82	1.5	Brown yellow turns yellow	4, 8
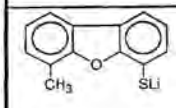 **L2-07**	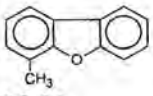	E + G	10.0; 1.82	2 + 15min	Orange	4, 8
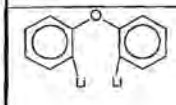 **L2-08**	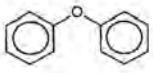	D	10.0; 1.70	3	Brown red precipitate	4

General method to prepare lithiated thiolates

Method G: After lithiation of the substrate, flowers of sulfur (0.32g, 10mmol) was added in one portion, stirred for the indicated time at -50°C or until all of the sulfur reacted. The solution was ready for subsequent reactions.

Method H: After lithiation of the substrate, flowers of sulfur (0.32g, 10mmol) was added in one portion at -10°C. After stirring for the indicated time at RT, the solution was ready for subsequent reactions.

Addition of a methyl substituent (**L2-07**)

Method I: After lithiation of the substrate, MeI (0.65ml, 10mmol) was added and stirred for 30 minutes at -30°C. The mixture was removed from the cold and allowed to raise room temperature and stirring was continued for another 12h. The yellow-white solution was poured into water and extracted with ether. The ether layers were dried over $MgSO_4$ and evaporated to give a yellow oil. Column chromatography on silica gel with 1:1 hexane:dichloromethane as eluent gave 1-methyldibenzofuran (first fraction), a yellow waxy compound (1.46g, 80.22%). Recrystallization

Table 6.2 Synthesis of heteroaromatic precursors used in this study.

Heteroaromatic Precursor/ Product	Starting Compound	Method	Amount of starting material (mmol; g)	Reaction time (h)	Colour and yield of product (g; %)	Reference
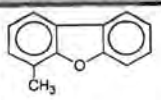 **L2-07**	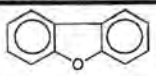 **L2-06**	A + I	10.0; 1.68	5 + 12	White waxy solid 1.46; 80.2	4, 8
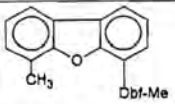 **L2-07b**	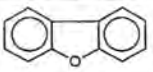 **L2-06**	A + I	10.0; 1.68	5 + 12	White waxy solid 1.46; 80.2	4, 8
 **L3-01**	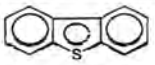 **L2-01**	F + H + J	10.0; 1.84	5 + 1	White-yellow solid 1,58; 73.2	4, 5, 8
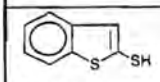 **L3-02**	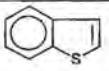 **L2-02**	A + G + J	10.0; 1.34	30min. + 20 min.	White-yellow solid 1.20; 72.5	4, 6
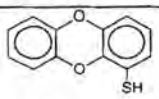 **L3-03**	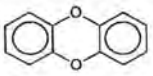 **L2-03**	B + G + J	10.0; 1.84	1 + 15min.	White-yellow solid 1,60; 74.1	4, 9
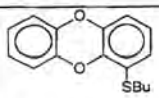 **L3-03b**	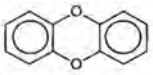 **L2-03**	B + G + J	10.0; 1.84	1 + 15min.	White-yellow solid 1,60; 74.1	4, 9
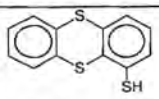 **L3-04**	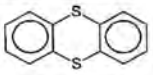 **L2-04**	B + G + J	10.0; 2.16	2 + 15min.	Pale yellow solid 1.78; 71.6	4, 10
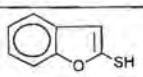 **L3-05**	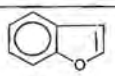 **L2-05**	C + G + J	10.0; 1.1ml	30min. + 20min.	White-yellow solid 1.06; 70.6	4, 5
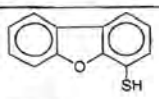 **L3-06**	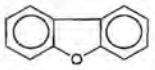 **L2-06**	A + G + J	10.0; 1.68	5 + 2	Pale yellow solid 1.52; 76.1	4, 7
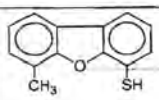 **L3-07**	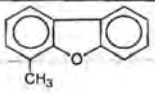 **L2-07**	E + G + J	10.0; 1.82	2 + 15min	Pale yellow solid 1.58; 73.8	4, 8

from dichloromethane yielded white crystals. *Anal.* Calc. for $C_{13}H_{10}O$: C, 85.68%; H, 5.54%. Found: C, 86.29%; H, 5.02%.

Protonation of lithiated heteroaromatic thiolates

Method J: To protonate the thiolates, HCl gas was bubbled through the solution for about 5 minutes. The solution turned into a pale yellow, milky colour and the solvent was evaporated under reduced pressure. The pale yellow residue was filtered through silica gel with dichloromethane and the resulting residue was again filtered with hexane to wash away the unreacted dibenzodioxin. Chromatography with dichloromethane:hexane (1:1) as eluent, gave a white-yellow product, which precipitated as soon as the solvent started evaporating. *Anal.* Calc. for **L3-01** $C_{12}H_8S_2$: C, 66.62%; H, 3.74%. Found: C, 66.86%; H, 3.49%. *Anal.* Calc. for **L3-02** $C_8H_6S_2$: C, 57.83%; H, 3.65%. Found: C, 58.27%; H, 3.98%. *Anal.* Calc. for **L3-03** $C_{12}H_8O_2S$: C, 66.35%; H, 6.31%. Found: C, 66.66%; H, 6.49%. *Anal.* Calc. for **L3-04** $C_{12}H_8S_3$: C, 57.83%; H, 3.65%. Found: C, 57.97%; H, 3.78%. *Anal.* Calc. for **L3-05** C_8H_6OS: C, 63.99%; H, 4.04%. Found: C, 64.37%; H, 4.39%. *Anal.* Calc. for **L3-06** $C_{12}H_8SO$: C, 71.99%; H, 4.04%. Found: C, 72.44%; H, 4.48%. *Anal.* Calc. for **L3-07** $C_{13}H_{10}OS$: C, 72.94%; H, 4.67%. Found: C, 73.56%; H, 4.89%.

6.3 Synthesis of titanocene derivatives

The synthesis of new titanocene derivatives follows a general method, but the resulting complexes and the purification of the complexes are very different. A general procedure is given in the shaded area and thereafter follows the remaining details for each reaction.

General method for synthesis of titanocene derivatives (unless indicated otherwise)

At -50°C the lithiated ligand mixture (Table 6.1) was added to a solution of titanocene dichloride (2.49g, 10.0mmol) in THF. A colour change of the reaction mixture was observed almost immediately and stirring was continued at -50°C for 30 minutes. The mixture was allowed to warm to room temperature and it was stirred for another 90 minutes. The solvent was evaporated and the residue was dissolved in dichloromethane and filtered through silica gel. The products were evaporated to dryness and the residue was stored under nitrogen at 5°C until it was subjected to purification. In all cases where column chromatography was used, the first fraction was colourless and was identified as unreacted heteroarene.

Synthesis of chlorobis(cyclopentadienyl)(dibenzofuran-4-yl)titanium(IV) **2-01** and bis(cyclopentadienyl)bis(dibenzofuran-4-yl)titanium(IV) **2-02**

2-01 **2-02**

The general method described above was followed for lithiated dibenzofuran. The mixture was stirred for 10h at –30°C during which the colour of the reaction mixture changed from bright red to orange. After filtering, an orange residue remained which was subjected to column chromatography with aluminium oxide and with a 1:1 THF:hexane mixture as eluent. The first fraction was unreacted dibenzofuran and the second yellow band that followed was isolated and characterized, yielding bis(cyclopentadienyl)bis(dibenzofuran-4-yl)titanium(IV) **2-02** (1.79g, 34.9%) *Anal.* Calc. for $C_{34}H_{24}O_2Ti$: C, 79.66%; H, 4.73%. Found: C, 79.04%; H, 4.26%. The desired product, chlorobis(cyclopentadienyl)(dibenzofuran-4-yl)titanium(IV) **2-01** (0.39g, 10.2%), was collected as an orange band. *Anal.* Calc. for $C_{22}H_{17}ClOTi$: C, 69.38%; H, 4.51%. Found: C, 69.45%; H, 4.67%. Recrystalization of **2-02** in hexane:dichloromethane yielded orange crystals suitable for single crystal X-ray diffraction studies.

Synthesis of chlorobis(cyclopentadienyl)(6-methyl dibenzofuran-4-yl)titanium(IV) **2-03** and bis(cyclopentadienyl)bis(6-methyl dibenzofuran-4-yl)titanium(IV) **2-04**

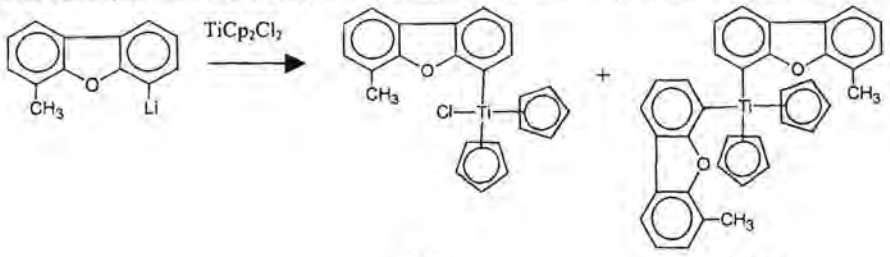

2-03 **2-04**

In this case the colour of the reaction mixture changed from bright red to yellow-brown. After filtering, an orange-brown residue was obtained which was subjected to column chromatography on silica gel and with a 7:1 hexane:THF mixture as eluent. The first fraction was a yellow band, identified as bis(cyclopentadienyl)bis(6-methyl dibenzofuran-4-yl)titanium(IV) **2-04** (2.27g, 42.0%). *Anal.* Calc. for $C_{36}H_{28}O_2Ti$: C, 79.97%; H, 5.23%. Found: C, 80.32%; H, 5.72%. An orange band followed, which was identified as the desired product chlorobis(cyclopentadienyl)(6-methyl

dibenzofuran-4-yl)titanium(IV) **2-03** (1.22g, 30.9%). *Anal.* Calc. for $C_{23}H_{19}ClOTi$: C, 69.95%; H, 4.86%. Found: C, 69.65%; H, 4.43%.

Synthesis of chlorobis(cyclopentadienyl)(dibenzodioxin-1-yl)titanium(IV) **2-05** and (μ-oxo)bis[bis(cyclopentadienyl)(dibenzodioxin-1-yl)titanium(IV)] **2-06**

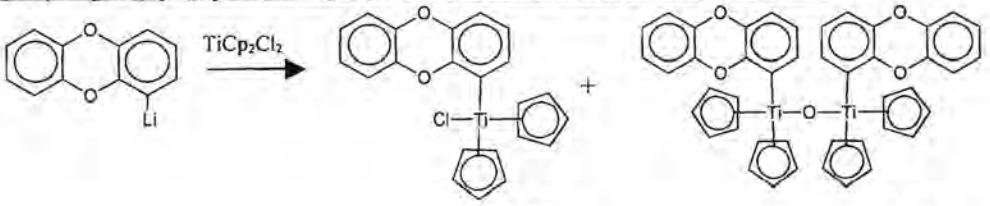

2-05 **2-06**

Following the general method with lithiated **L2-03** the colour of the reaction mixture changed from bright red to clear orange-brown and then to dark orange-brown. After filtering, the remaining orange residue was subjected to column chromatography on silica gel and with a 6:4 hexane:dichloromethane mixture as eluent. The desired product was obtained from an orange fraction, chlorobis(cyclopentadienyl)(dibenzodioxin-1-yl)titanium(IV) **2-05**. (Yield: 1.47g, 37.1%). Recrystallization from hexane/THF (1:1) gave bright orange, diamond shaped crystals with the solvents co-precipitating (mp.: 92°C). *Anal.* Calc. for $C_{22}H_{17}ClO_2Ti \cdot C_6H_{14} \cdot C_4H_8O$: C, 69.24%; H, 7.10%. Found: C, 69.45%; H, 7.22%. A yellow fraction was collected before the major product, but turned black on attempts to filter it with dichloromethane. Finally, a yellow product, (μ-oxo)bis[bis(cyclopentadienyl)(dibenzodioxin-1-yl)titanium(IV)] **2-06**, was collected by extracting and filtrating the black residue with benzene. (Yield: 2.07g, 28.0%). *Anal.* Calc. for $C_{44}H_{34}O_5Ti_2$: C, 71.53%; H, 4.65%. Found: C, 71.95%; H, 4.82%.

Synthesis of (benzofuran-2-yl)chlorobis(cyclopentadienyl)titanium(IV) **2-07**

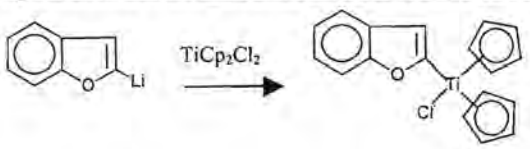

2-07

Following the general method with lithiated **L2-05** the colour of the reaction mixture changed from bright red to bright orange. Due to decomposition on silica gel, an aluminium oxide filter was used instead and a bright red orange residue was obtained. The residue was subjected to column chromatography with aluminium oxide and with a 2:1 hexane:dichloromethane mixture as eluent. The first fraction was unreacted benzothiophene. The desired product, (benzofuran-2-yl)chlorobis(cyclopentadienyl)titanium(IV) **2-07** (1.49g, 45.0%), followed as a red-orange band. The

product was highly unstable and decomposed in air and at room temperature. It could be retained for only one week under argon at 5°C.

Synthesis of chlorobis(cyclopentadienyl)(dibenzothiophen-4-yl)titanium(IV) **2-08**

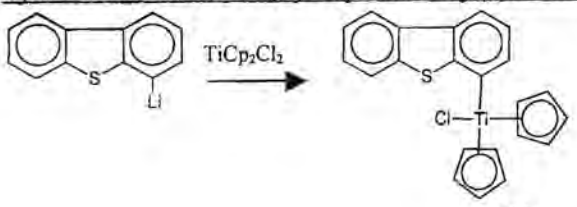

2-08

The general method was followed using lithiated L2-01. The mixture **was** stirred at **–60°C** during which time the colour of the reaction mixture changed from bright red to orange. After filtering, an orange residue remained which was subjected to column chromatography on silica gel with a 2:1 dichloromethane:hexane mixture as eluent. The desired product was isolated from an orange band, chlorobis(cyclopentadienyl)(dibenzothiophen-4-yl)titanium(IV) **2-08** (2.07g, 52.2%). *Anal.* Calc. for $C_{22}H_{17}ClSTi$: C, 66.60%; H, 4.33%. Found: C, 67.02%; H, 4.67%.

Synthesis of chlorobis(cyclopentadienyl)(thianthren-1-yl)titanium(IV) **2-09** and (μ-oxo)bis[bis(cyclopentadienyl)(thianthren-1-yl)titanium(IV)] **2-10**.

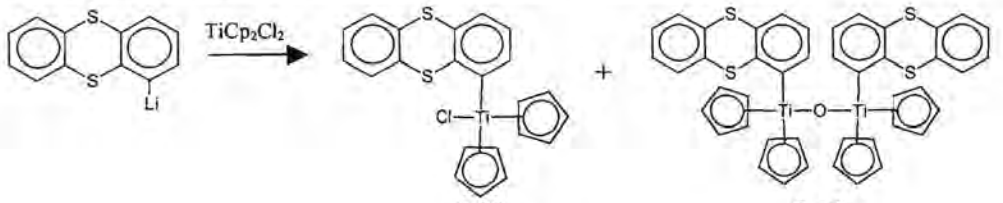

2-09 **2-10**

Using lithiated **L2-04** the mixture was stirred at RT for 2h. The colour of the reaction mixture changed from bright red to clear red-brown. After filtering an orange residue was left which was subjected to column chromatography on silica gel and with a 6:4 hexane:dichloromethane mixture as eluent. The desired product was isolated and characterized from an orange fraction to give, chlorobis(cyclopentadienyl)(thianthren-1-yl)titanium(IV) **2-09**. (Yield: 1.59g, 37.1%). Product **2-09** quickly converted to (μ-oxo)bis[bis(cyclopentadienyl)(thianthren-1-yl)titanium(IV)] **2-10**, a yellow band. (Yield: 2.51g, 31.3%). *Anal.* Calc. for $C_{44}H_{34}S_4OTi_2$: C, 65.83%; H, 4.28%. Found: C, 66.15%; H, 4.52%.

Synthesis of bis(cyclopentadienyl)(diphen-2,2′-yl ether)titanium(IV) **2-11**

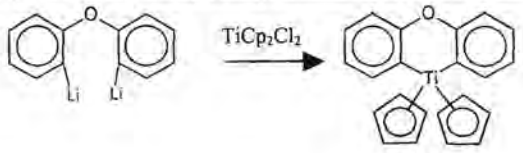

2-11

Following the general method with lithiated **L2-08** the colour of the reaction mixture changed from bright red to orange. After filtering an orange residue was subjected to column chromatography on silica gel and with a 1:1 hexane:dichloromethane mixture as eluent. The first yellow band was discarded and an orange band gave the expected product, bis(cyclopentadienyl)(diphen-2,2′-yl ether)titanium(IV) **2-11** (1.32g, 38.1%). *Anal.* Calc. for $C_{22}H_{18}OTi$: C, 76.30%; H, 5.25%. Found: C, 76.95%; H, 5.72%. The product was an oily residue.

Synthesis of chlorobis(cyclopentadienyl)(dibenzofuran-4-ylsulfanyl)titanium(IV) **3-01** and bis(cyclopentadienyl)bis(dibenzofuran-4-ylsulfanyl)titanium(IV) **3-02**

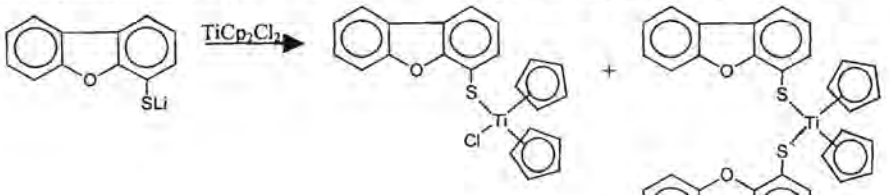

3-01 **3-02**

Following the general method with lithiated **L3-06** the colour of the reaction mixture changed from bright red to purple. After filtering, a purple residue was subjected to column chromatography with silica gel and with a 3:2 hexane:dichloromethane mixture as eluent. The first fraction gave the expected red-orange product, chlorobis(cyclopentadienyl)(dibenzofuran-4-ylsulfanyl)titanium(IV) **3-01** (1.21g, 29.3%). *Anal.* Calc. for $C_{22}H_{17}ClOSTi$: C, 64.00%; H, 4.16%. Found: C, 64.85%; H, 4.22%. An unidentified pink fraction was followed by a purple band, bis(cyclopentadienyl)bis(dibenzofuran-4-ylsulfanyl)titanium(IV) **3-02** (2.33g, 40.4%). *Anal.* Calc. for $C_{34}H_{24}O_2S_2Ti$: C, 70.22%; H, 4.20%. Found: C, 69.35%; H, 3.72%.

Synthesis of chlorobis(cyclopentadienyl)(6-methyl dibenzofuran-4-ylsulfanyl)titanium(IV) **3-03** and bis(cyclopentadienyl)bis(6-methyl dibenzofuran-4-ylsulfanyl)titanium(IV) **3-04**

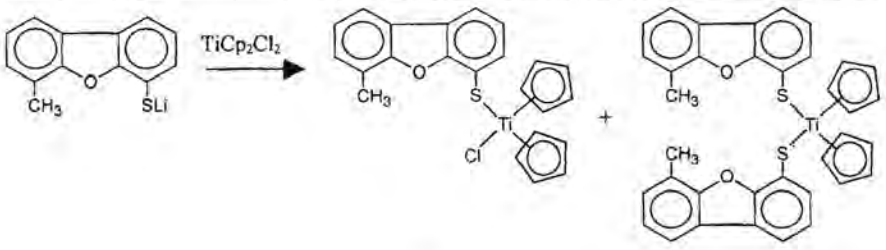

3-03 **3-04**

Following the general method for lithiated **L3-07** the colour of the reaction mixture changed from bright red to dark red. After filtering a dark red residue was obtained which was subjected to column chromatography on silica gel and with a 1:1 hexane:dichloromethane mixture as eluent. The first band contained very little of an unidentified purple product and the next fraction gave the expected product which was isolated from a red band, chlorobis(cyclopentadienyl)(6-methyl dibenzofuran-4-ylsulfanyl)titanium(IV) **3-03** (1.29g, 30.2%) *Anal.* Calc. for $C_{23}H_{19}ClOSTi$: C, 64.71%; H, 4.30%. Found: C, 65.02%; H, 4.52%. A purple product followed yielding bis(cyclopentadienyl)bis(6-methyl dibenzofuran-4-ylsulfanyl)titanium(IV) **3-04** (2.11g, 34.9%). *Anal.* Calc. for $C_{36}H_{28}O_2S_2Ti$: C, 71.51%; H, 4.68%. Found: C, 71.95%; H, 5.02%.

Synthesis of chlorobis(cyclopentadienyl)(dibenzodioxin-1-ylsulfanyl)titanium(IV) **3-05** and bis(cyclopentadienyl)bis(dibenzodioxin-1-ylsulfanyl)titanium(IV) **3-06**

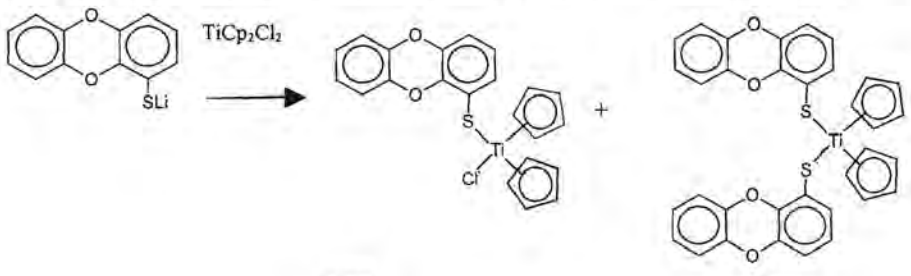

3-05 **3-06**

By using lithiated **L3-03** the colour of the reaction mixture changed from red to dark red. After filtering a red-purple residue remained which was subjected to column chromatography on silica gel and with a 1:1 hexane:dichloromethane mixture as eluent. First a red-purple band was collected and gave bis(cyclopentadienyl)bis(dibenzodioxin-1-ylsulfanyl)titanium(IV) **3-06** (1.27 g, 22.0%; mp. = 189°C). *Anal.* Calc. for $C_{34}H_{24}O_4STi$: C, 67.11%; H, 3.98%. Found: C, 67.39%; H, 4.11%. The last fraction afforded chlorobis(cyclopentadienyl)(dibenzodioxin-1-ylsulfanyl)titanium(IV) **3-05** (0.77 g,

17.9%) from a red zone on the column. *Anal.* Calc. for $C_{22}H_{17}ClO_2STi$: C, 61.63%; H, 4.00%. Found: C, 62.09%; H, 4.23%.

Synthesis of (benzofuran-2-ylsulfanyl)chlorobis(cyclopentadienyl)titanium(IV) **3-07** and bis(cyclopentadienyl)bis(benzofuran-2-ylsulfanyl)titanium(IV) **3-08**

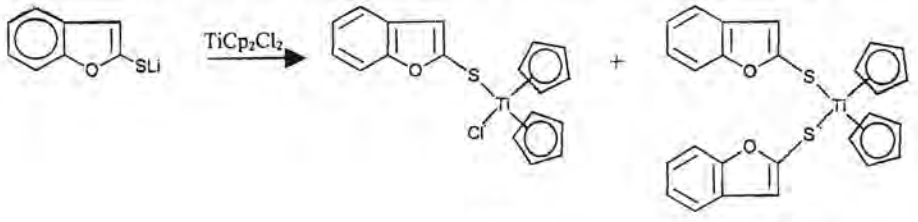

3-07 **3-08**

Following the general method with lithiated **L3-05** the colour of the reaction mixture changed from bright red to purple. After filtering a purple residue was subjected to column chromatography on silica gel and with a 2:3 hexane:dichloromethane mixture as eluent. The first fraction gave unreacted benzofuran and the second fraction afforded the blue-purple product, bis(cyclopentadienyl)bis (benzofuran-2-ylsulfanyl)titanium(IV) **3-08** (1.95g, 41.0%). *Anal.* Calc. for $C_{26}H_{20}O_2S_2Ti$: C, 65.54%; H, 4.24%. Found: C, 66.05%; H, 4.52%. The desired product was obtained next from a red-purple band on the column (benzofuran-2-ylsulfanyl)chlorobis(cyclopentadienyl) titanium(IV) **3-07** (1.07g, 29.5%). *Anal.* Calc. for $C_{18}H_{15}ClOSTi$: C, 59.59%; H, 4.18%. Found: C, 60.75%; H, 4.42%. Recrystalization of **3-08** from a hexane:dichloromethane mixture yielded dark purple crystals suitable for single crystal X-ray diffraction studies.

Synthesis of chlorobis(cyclopentadienyl)(dibenzothien-4-ylsulfanyl)titanium(IV) **3-09** and bis(cyclopentadienyl)bis(dibenzothien-4-ylsulfanyl)titanium(IV) **3-10**

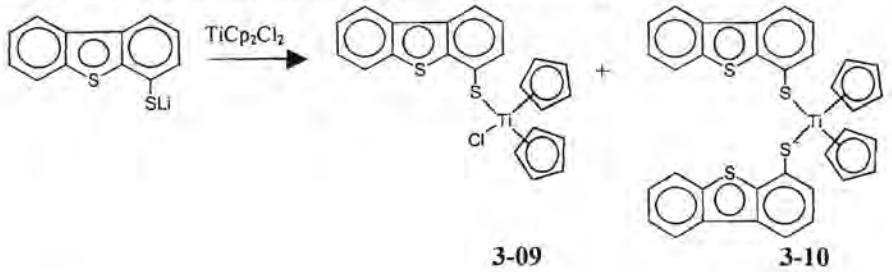

3-09 **3-10**

By using lithiated **L3-01** the colour of the reaction mixture changed from bright red to deep red. After filtering a red residue was obtained which was subjected to column chromatography on silica gel and with a 2:1 hexane:dichloromethane mixture as eluent. The first fraction collected was a purple band yielding bis(cyclopentadienyl)bis(dibenzothien-4-ylsulfanyl)titanium(IV) **3-10** (2.48g, 40.7%). *Anal.*

Calc. for $C_{34}H_{24}S_4Ti$: C, 67.10%; H, 3.98%. Found: C, 65.55%; H, 3.67%. The desired product was purified from a red band to give chlorobis(cyclopentadienyl)(dibenzothien-4-ylsulfanyl)titanium(IV) **3-09** (1.20g, 28.0%). *Anal.* Calc. for $C_{22}H_{17}ClS_2Ti$: C, 61.61%; H, 4.00%. Found: C, 61.85%; H, 4.42%. Recrystalization of **3-09** from a hexane:dichloromethane mixture yielded deep red crystals suitable for single crystal X-ray diffraction studies.

Synthesis of chlorobis(cyclopentadienyl)(thianthren-1-ylsulfanyl)titanium(IV) **3-11** and bis(cyclopentadienyl)bis(thianthren-1-ylsulfanyl)titanium(IV) **3-12**

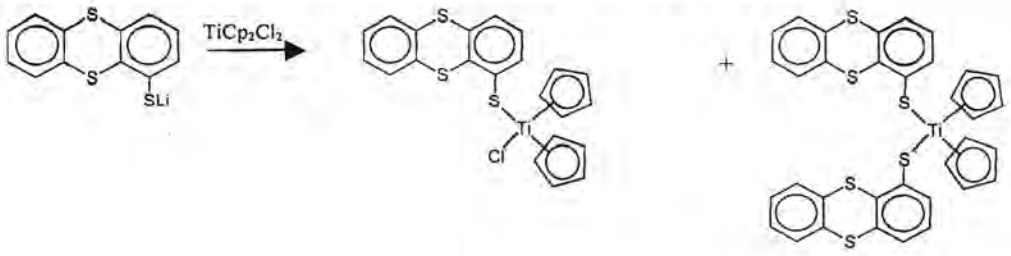

3-11 **3-12**

Following the general method with lithiated **L3-03** the colour of the reaction mixture changed from red to dark red. After filtering a red-purple residue was obtained which was subjected to column chromatography on silica gel and with a 6:4 hexane:dichloromethane mixture as eluent. First a red-purple band was collected, affording bis(cyclopentadienyl)bis(thianthren-1-ylsulfanyl)titanium(IV) **3-12** (1.41 g, 21.0%). *Anal.* Calc. for $C_{34}H_{24}S_6Ti$: C, 60.63%; H, 3.60%. Found: C, 60.89%; H, 3.91%. A later fraction yielded chlorobis(cyclopentadienyl)(thianthren-1-ylsulfanyl)titanium(IV) **3-11** (0.83 g, 18%) from a red band on the column. *Anal.* Calc. for $C_{22}H_{17}ClS_3Ti$: C, 57.34%; H, 3.73%. Found: C, 57.69%; H, 3.93%.

Synthesis of (benzothien-2-ylsulfanyl)chlorobis(cyclopentadienyl)titanium(IV) **3-13** and bis(cyclopentadienyl)bis(benzothien-2-ylsulfanyl)titanium(IV) **3-14**

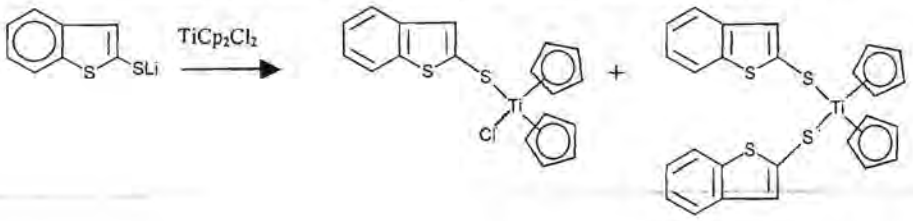

3-13 **3-14**

Following the general method with lithiated **L3-06** the colour of the reaction mixture changed from bright red to dark red. After filtering, a dark red residue was obtained which was subjected to column

chromatography on silica gel and with a 1:1 petroleum ether:dichloromethane mixture as eluent. The first fraction, a purple band, gave bis(cyclopentadienyl)bis(benzothien-2-ylsulfanyl)titanium(IV) **3-14** delete formula (2.48g, 48.8%). *Anal.* Calc. for $C_{26}H_{20}S_4Ti$: C, 61.41%; H, 3.97%. Found: C, 61.75%; H, 4.12%. The desired product was isolated from a red band (benzothien-2-ylsulfanyl)chlorobis(cyclopentadienyl)titanium(IV) **3-13** (1.33g, 35.1%). *Anal.* Calc. for $C_{18}H_{15}ClS_2Ti$: C, 57.07%; H, 4.00%. Found: C, 57.25%; H, 4.22%.

6.4 Synthesis of bi- and trinuclear complexes

The synthesis of homobinuclear and heterotrinuclear complexes require (i) the synthesis of a suitable connecting molecule with appropriate metal bonding functions to act as a bridging ligand between the metal centra and (ii) the introduction of metal substrates designed to preferably coordinate to fixed positions on this ligand.

Synthesis of bridging ligands

Synthesis of 2-({2-[(2-mercaptoethyl)methylamino]ethyl}methylamino)ethanethiol [$C_8H_{20}N_2S$] **L4-04**

L4-03 **L4-04**

This synthesis was based on a method in literature, which was slightly modified[9]. N,N-dimethyl ethylene diamine **L4-03** (2.40g, 27.3mmol) was dissolved in dry toluene and thiiran (5.00ml, 83.0mmol), dissolved in dry toluene, was added dropwise at 50°C. It was immediately sealed in a pressure tube and heated to 110°C. After 5h the tube was cooled to RT and the solution was filtered to remove the polymer. The toluene was evaporated to give a pale yellow oil and distillation (110 - 120°C) under reduced pressure gave product **L4-04** (2.69g, 47.4%) as a colourless oil. *Anal.* Calc. for $C_8H_{20}N_2S_2$: C, 46.13%; H, 9.70%; N, 13.44%. Found: C, 49.01%; H, 9.43%; N, 13.85%.

Synthesis of 2-(2-methylamino ethylamino)ethanethiol [$C_5H_{14}N_2S$] **L4-05**

L4-02 **L4-05**

9. C. Marabella, J. Enemark, A. Miller, A. Bruce, N .Pariyadath, J, Corbin, E. Stiefel, *J. Org. Chem.*, **1983**, *22*, 3456.

The method for **L4-04** was followed with N-methyl ethylene diamine **L4-02** (2.80g, 40.0mmol) and thiiran (2.80ml, 46.7mmol). The crude pale yellow oil was distilled (97 - 105°C) and gave product **L4-05** (2.75g, 51.3%) as a colourless oil. *Anal.* Calc. for $C_5H_{14}N_2S$: C, 44.75%; H, 10.54%; N, 20.87%. Found: C, 47.55%; H, 9.96%; N, 20.32%.

Synthesis of N,N′-bis-(3-cyclopenta-2,4-dienyl propyl) ethylene diamine **L4-07**

(a) Synthesis of 3-cyclopenta-2,4-dienyl propionaldehyde **L4-06**

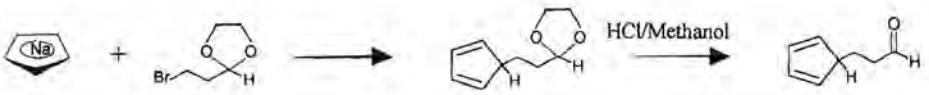

L4-06

NaCp (4.40g, 50.0mmol) was dissolved in THF and 2-(2-bromoethyl)-[1,3]-dioxolan (9.05g, 50.0mmol) was added and stirred for 4h at RT. The colour of the reaction mixture changed from purple to brown. The THF was evaporated and the residue was treated with a mixture of diluted HCl (1 part HCl in 3 parts distilled water) and methanol in a 1:1 ratio. The mixture was stirred for 1h at RT and the product was extracted from the water with diethyl ether. After evaporation a brown oil 3-cyclopenta-2,4-dienyl propionaldehyde **L4-06** (1.32g, 54.1%) remained and this product was used without further purification. *Anal.* Calc. for $C_8H_{10}O$: C, 78.64%; H, 8.27%. Found: C, 78.97%; H, 8.53%.

(b) Synthesis of N,N′-bis-(3-cyclopenta-2,4-dienyl propyl) ethylene diamine **L4-07**

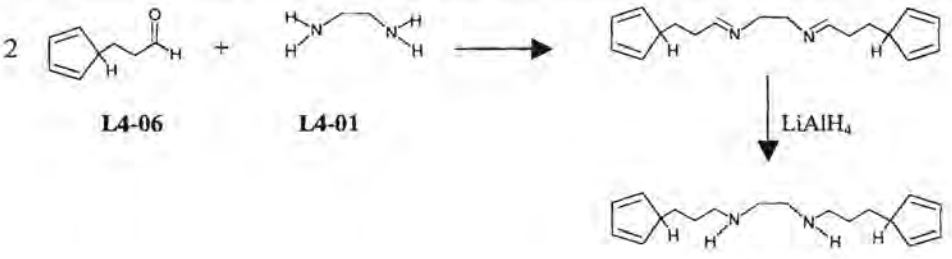

L4-06 **L4-01**

L4-07

L4-06 (2.40g, 20.0mmol) was dissolved in benzene and **L4-01** (0.78g, 10mmol) was added. The mixture was refluxed overnight under argon in a Dean-Stark apparatus. The water that formed during the first two hours of reflux was removed. After the reaction was completed the benzene was removed to leave a dark brown residue, which was dissolved in THF at RT. Lithium aluminium hydride (0.82g, 20mmol) was added in small portions and the mixture was stirred for 1h. The grey sticky mixture was

treated with 1ml of distilled water, then with 1ml 15% KOH solution and finally with 3ml distilled water. The mixture was filtered and evaporated to leave a brown residue. The residue was dissolved in the minimum dichloromethane whereafter hexane was added. The solution was filtered and the filtrate was evaporated to dryness to yield a yellow-brown oil that was identified as the product N,N′-bis-(3-cyclopenta-2,4-dienyl propyl) ethylene diamine **L4-07** (1.49g, 51.5%). *Anal.* Calc. for $C_{18}H_{28}N_2$: C, 46.31%; H, 10.38%; N, 10.28%. Found: C, 44.56%; H, 10.98%; N, 9.72%.

Synthesis of N-(3-cyclopenta-2,4-dienyl propyl)-N′-methyl ethylene diamine **L4-08**

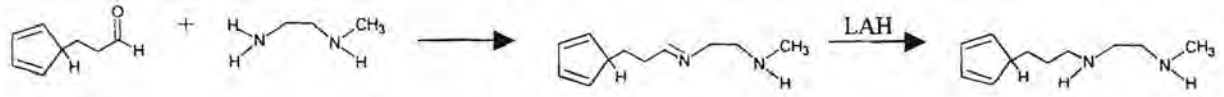

L4-06 **L4-02** **L4-08**

The procedure for **L4-07** was repeated with **L4-06** (2.03g, 17.0mmol) and **L4-02** (0.70g, 17mmol) instead. The reduction was done with $LiAlH_4$ (0.70g, 17mmol) and after extraction and filtration a yellow-brown oil was isolated and identified as the product N-(3-cyclopenta-2,4-dienyl propyl)-N′-methyl ethylene diamine **L4-08** (1.62g, 53.5%). *Anal.* Calc. for $C_{11}H_{18}N_2$: C, 74.10%; H, 10.20%; N, 15.70%. Found: C, 74.46%; H, 10.38%; N, 15.92%.

Synthesis of metal complexes

The general procedure for the addition of $K_2[PtCl_4]$ is given below in the shaded area. The introduction of the titanium fragment was achieved by using titanocene dichloride or trichloro cyclopentadienyl titanium (IV).

$K_2[PtCl_4]$ (0.42g, 1,0 mmol) was dissolved in the minimum of hot distilled water and the ligand was dissolved in acetonitrile. The latter was added to the platinum solution at RT. A colour change of the solution was observed and the mixture was stirred for 24 h at RT. The precipitate that formed was collected and dried.

Synthesis of $[\{\mu\text{-}C_8H_{18}N_2O_2\}Ti_2Cp_4Cl_2]$ **4-01**

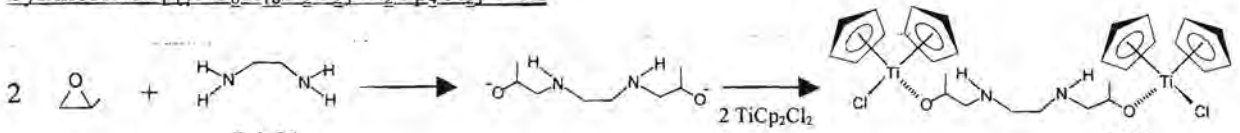

L4-01 **4-01**

L4-01 (0.78g, 10mmol) was dissolved in THF and methyl epoxide (1.4ml, 20mmol) was added dropwise at RT while stirring. After stirring for 24h at RT the solution remained colourless. At -50°C titanocene dichloride (4.98g, 20.0mmol) was added and the solution was stirred for 30 minutes. After heating to RT the solution was stirred for 4 days. The colour changed from red-orange to yellow. The THF was evaporated and the residue was dissolved in hot toluene and filtered. The filtrate was concentrated and mixed with hexane causing a yellow precipitate to form, which was identified as $[\{\mu\text{-}C_8H_{18}N_2O_2\}Ti_2Cp_4Cl_2]$ **4-01** (1.51g, 25.1%). *Anal.* Calc. for $C_{28}H_{38}Cl_2N_2O_2Ti_2$: C, 55.89%; H, 6.38%; N, 4.65%. Found: C, 59.45%; H, 6.12%; N, 4.12%.

Synthesis of $[TiCp_2(OC_6H_{15}N_2)Cl]$ **4-02**

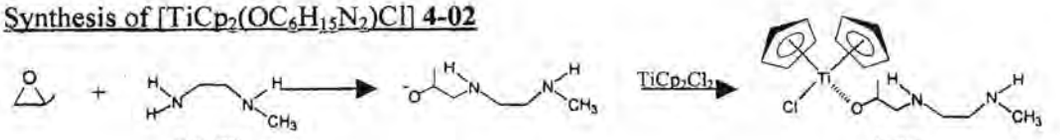

L4-02 **4-02**

The procedure for **4-01** was repeated with **L4-02** (0.74g, 10mmol) and methyl oxiran (0.70ml, 10mmol). Addition of titanocene dichloride (2.49g, 10.0mmol) changed the colour from red to orange. The yellow precipitate was identified as $[TiCp_2(OC_6H_{15}N_2)Cl]$ **4-02** (1.00g, 29.2%). *Anal.* Calc. for $C_{16}H_{23}ClN_2OTi$: C, 56.12%; H, 6.78%; N, 8.17%. Found: C, 60.42%; H, 6.22%; N, 7.82%.

Synthesis of $[\{\mu\text{-}C_8H_{18}N_2S_2\}Ti_2Cp_4Cl_2]$ **4-03**

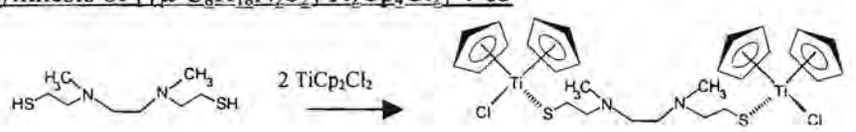

L4-04 **4-03**

Titanocene dichloride (2.49g, 10.0mmol) was dissolved in THF and added to a solution of **L4-03** (1.04g, 5.00mmol) in THF at -50°C. The solution was stirred for 30 minutes at -50°C and after heating to RT stirring was continued for 24h. The colour changed from bright to red-orange. The THF was evaporated and the residue was dissolved in dichloromethane and filtered. The filtrate was concentrated and mixed with hexane causing an orange-red precipitate to form, which was identified as $[\{\mu\text{-}C_8H_{18}N_2S_2\}Ti_2Cp_4Cl_2]$ **4-03** (1.56g, 24.6%). *Anal.* Calc. for $C_{28}H_{38}Cl_2N_2S_2Ti_2$: C, 53.07%; H, 6.06%; N, 4.42%. Found: C, 55.65%; H, 6.29%; N, 4.02%.

Synthesis of [$TiCp_2(C_6H_{15}N_2S)Cl$] **4-04**

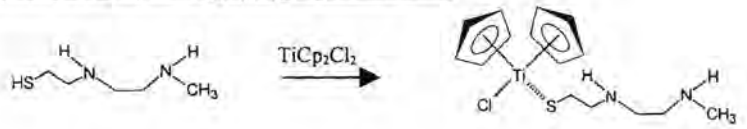

L4-05 **4-04**

The same procedure was followed as for **4-03**, but with titanocene dichloride (0.75g, 3.0mmol) and **L4-05** (0.40g, 3.0mmol). The colour changed from bright to red-orange. From the filtrate an orange-red precipitate was collected, which was identified as [$TiCp_2(SC_6H_{15}N_2)Cl$] **4-04** (0.31g, 29.7%). *Anal.* Calc. for $C_{15}H_{23}ClN_2STi$: C, 52.01%; H, 6.71%; N, 8.08%. Found: C, 57.56%; H, 6.85%; N, 7.72%.

Synthesis of [$Pt(N,N'\text{-}C_{18}H_{28}N_2)Cl_2$] **4-05**

L4-07 **4-05**

The general method for addition of $K_2[PtCl_4]$ to **L4-07** (1.00g, 4.00mmol) was followed whereby the colour changed from red via brown to yellow-brown. After the reaction was completed a pink precipitate separated from the brown solution. The pink precipitate was identified as [$Pt(N,N'\text{-}C_{18}H_{28}N_2)Cl_2$] **4-05** (0.83g, 39.7%). *Anal.* Calc. for $C_{18}H_{28}Cl_2N_2Pt$: C, 23.43%; H, 5.25%; N, 5.20%. Found: C, 21.58%; H, 4.96%; N, 4.97%.

Synthesis of [$Pt(N,N'\text{-}C_{11}H_{20}N_2)Cl_2$] **4-06**

L4-08 **4-06**

Following the general method for addition of $K_2[PtCl_4]$ (1.25g, 3.00mmol) to **L4-08** (0.54g, 3.00mmol) the colour of the reaction mixture changed from red to brown to pale brown. After the reaction was completed a pale pink-brown precipitate was separated from the brown solution. The pink-brown precipitate was identified as the product [$Pt(\mu\text{-}N,N'\text{-}C_{11}H_{20}N_2)Cl_2$] **4-06** (2.87g, 42.5 %). *Anal.* Calc. for $C_{11}H_{20}Cl_2N_2Pt$: C, 29.74%; H, 4.09%; N, 6.30%. Found: C, 30.04%; H, 4.29%; N, 6.52%.

Synthesis of $[\{\mu\text{-}\eta^5,\eta^5\text{-}C_{18}H_{26}N_2\}Ti_2Cp_2Cl_4]$ **4-07**

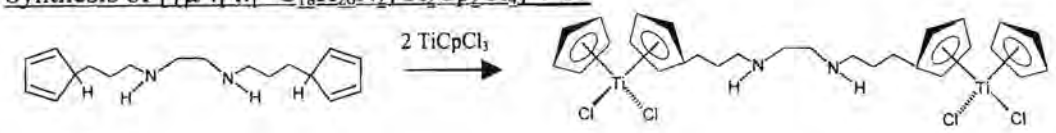

L4-07 **4-07**

L4-07 (1.38g, 5.00mmol) was dissolved in THF and added to NaH (0.24g, 10mmol) at RT. After stirring overnight the colour of the reaction mixture changed from yellow to brown. At -50°C trichlorocyclopentadienyltitanium (IV) (2.19g, 10.0mmol) was added and the solution was stirred for 30 minutes. After heating to RT the solution was stirred for 5h. The colour of the solution changed to dark brown. The THF was evaporated and the residue was dissolved in hot toluene and filtered. The volume of toluene was reduced and hexane was added until precipitation was completed. After filtration the yellow filtrate was collected and the solvent removed under reduced pressure. The residue was dissolved in dichloromethane. Addition of hexane precipitated a yellow product that was identified as $[\{\mu\text{-}\eta^5,\eta^5\text{-}C_{18}H_{26}N_2\}Ti_2Cp_2Cl_4]$ **4-07** (2.30g, 29.4%). *Anal.* Calc. for $C_{28}H_{36}Cl_4N_2Ti_2$: C, 52.66%; H, 5.69%; N, 4.38%. Found: C, 53.05%; H, 5.92%; N, 4.67%.

Synthesis of $[Ti_2\{\mu\text{-}\eta^5,\eta^5\text{-}(Pt(N,N'\text{-}C_{18}H_{26}N_2)Cl_2)\}Cp_2Cl_4]$ **4-08**

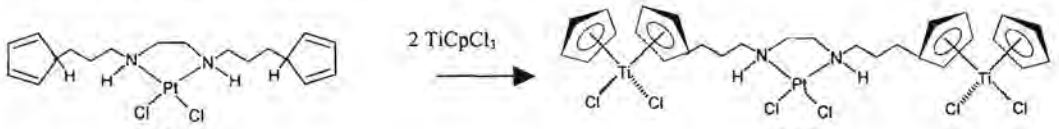

4-05 **4-08**

4-05 (0,13g, 0.25mmol) was dissolved in THF and added to NaH (0.01g, 0.5mmol) at RT. After stirring overnight at RT the colour of the reaction mixture changed from pink to brown-pink. At -50°C trichloro cyclopentadienyl titanium(IV) (0.10g, 0.50mmol) was added and the solution was stirred for 30 minutes. After heating to RT the solution was stirred for 24h. The colour of the solution changed to yellow and a cream-pink precipitate formed. The cream-pink product was identified as $[Ti_2\{\mu\text{-}\eta^5,\eta^5\text{-}(Pt(N,N'\text{-}C_{18}H_{26}N_2)Cl_2)\}Cp_2Cl_4]$ **4-08** (0.07g, 31.0%). *Anal.* Calc. for $C_{28}H_{36}Cl_6N_2Ti_2Pt$: C, 37.17%; H, 4.02%; N, 3.10%. Found: C, 37.45%; H, 4.42%; N, 3.41%. Attempts to synthesize this product by adding the metal substrates in the reverse order, i.e. the addition of $K_2[PtCl_4]$ to **4-07**, was unsuccessful.

Synthesis of $[\{\mu\text{-}\eta^5,\eta^5\text{-}C_{14}H_{16}\}Ti_2Cp_2Cl_4]$ **4-09**

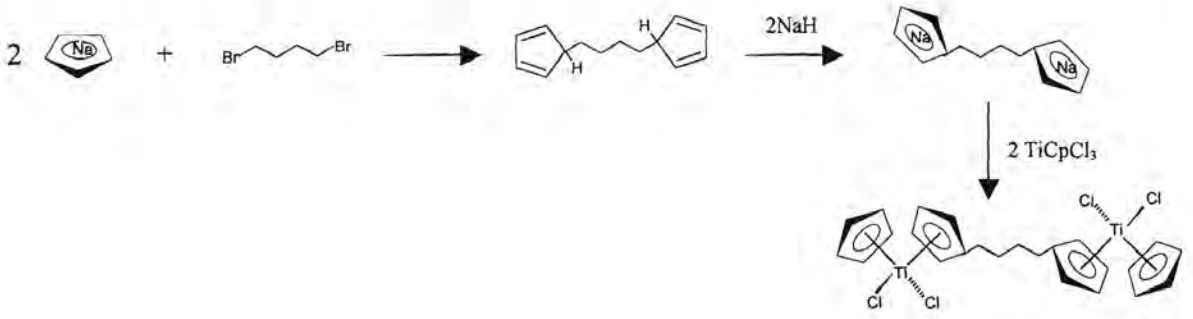

4-09

NaCp (4.40g, 50.0mmol) was dissolved in THF and added to 1,4-dibromobutane (5.40g, 25.0mmol) at RT. After stirring for 2h the pink-brown mixture was treated with NaH (1.20g for 60 % pure mixture, 50.0mmol) and stirred overnight. The resulting brown solution was then added to trichloro cyclopentadienyl titanium (IV) (10.95g, 50.00mmol,) dissolved in THF at RT. After stirring for 2h, the brown solution was evaporated to dryness and the residue was washed with 1 mol/dm^3 HCl solution, then with ethanol and finally with diethyl ether. After drying a dark green solid remained, which was identified as the product $[\{\mu\text{-}\eta^5,\eta^5\text{-}C_{14}H_{16}\}Ti_2Cp_2Cl_4]$ **4-09** (11.04g, 80.0%). *Anal.* Calc. for $C_{24}H_{26}Cl_4Ti_2$: C, 52.17%; H, 4.75%. Found: C, 52.61%; H, 4.92%.

Derivatives of **4-09** were synthesized according to the general method given in the shaded area below. The procedures for the preparation of the lithiated heteroaromatic substrates are given in Table 6.1.

General method for replacing Cl with a heteroaromatic ring ligand

At -50°C the lithiated heteroaromatic substrate was added to a solution of **4-09** (5.52g, 10.0mmol) in THF. A colour change of the reaction mixture was observed almost immediately and stirring was continued at -50°C for 30 minutes. The mixture was allowed to warm to room temperature and it was stirred for another 90 minutes. The solvent was evaporated and the residue was purified using extraction. The products were stored under nitrogen at 5°C.

Synthesis of $[\{\mu\text{-}\eta^5,\eta^5\text{-}C_{14}H_{16}\}Ti_2(Dbf)Cp_2Cl_3]$ **4-10**

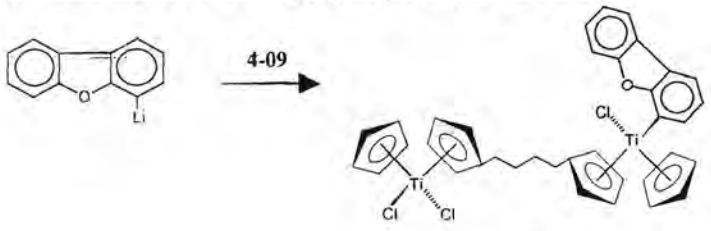

4-10

Following the general method with 10.0mmol of the lithiated dibenzofuran, the colour of the reaction mixture changed from dark green to green. The green residue was washed with hexane. The product was extracted using diethyl ether to give a green-yellow solution, which was evaporated to dryness to give $[\{\mu\text{-}\eta^5,\eta^5\text{-}C_{14}H_{16}\}Ti_2(Dbf)Cp_2Cl_3]$ **4-10** (2.76g, 40.3%). *Anal.* Calc. for $C_{36}H_{33}Cl_3OTi_2$: C, 63.24%; H, 4.88%. Found: C, 63.75%; H, 5.02%.

Synthesis of $[\{\mu\text{-}\eta^5,\eta^5\text{-}C_{14}H_{16}\}Ti_2(Dbf\text{-}S)Cp_2Cl_3]$ **4-11**

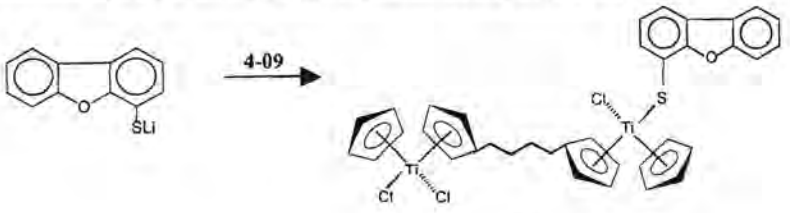

4-11

Following the general method with 10.0mmol of dibenzofuran-4-ylthiolate, the colour of the reaction mixture changed from dark green to brown-yellow. The brown residue was washed with hexane and a brown residue remained. The product was extracted from the residue by using diethyl ether to give an orange-yellow solution, which was evaporated to dryness to give an orange-yellow solid, $[\{\mu\text{-}\eta^5,\eta^5\text{-}C_{14}H_{16}\}Ti_2(Dbf\text{-}S)Cp_2Cl_3]$ **4-11** (3.15g, 44.0%). *Anal.* Calc. for $C_{36}H_{33}Cl_3OSTi_2$: C, 60.41%; H, 4.66%. Found: C, 60.80%; H, 4.82%.

Synthesis of $[\{\mu\text{-}\eta^5,\eta^5\text{-}C_{14}H_{16}\}\{Ti(Dbf\text{-}S)CpCl\}_2]$ **4-12**

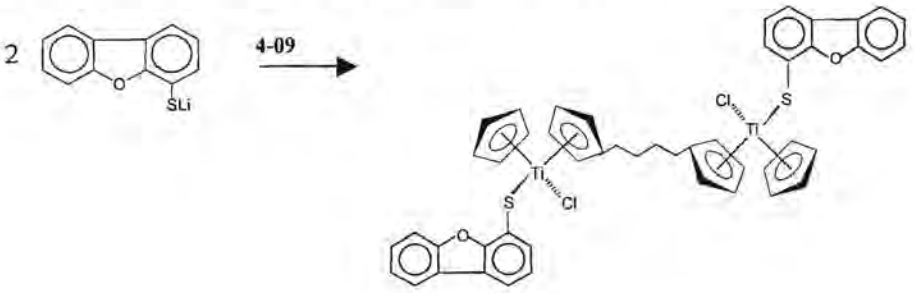

4-12

Following the general method with 20.0mmol of the dibenzofuran-4-ylthiolate, the colour of the solution changed from dark green to red. The green residue was washed with hexane and a purple residue remained. The residue was subjected to column chromatography on silica gel by starting with 1:1 hexane:dichloromethane mixture as eluent and increasing the polarity with time. The purple fraction was identified as $[\{\mu\text{-}\eta^5,\eta^5\text{-}C_{14}H_{16}\}\{Ti(Dbf\text{-}S)CpCl\}_2]$ **4-12** (3.16g, 35.9%). *Anal.* Calc. for $C_{48}H_{40}Cl_2O_2S_2Ti_2$: C, 65.52%; H, 4.59%. Found: C, 65.88%; H, 4.80%.

6.5 *In vitro* tests

The *in vitro* tests were executed using cell cultures with CoLo (colorectal carcinoma) cells and HeLa (human cervix epithelioid carcinoma) cells. The cells were incubated in an oven at 37 °C for 3h and the cell concentration was determined on day 0 by counting the cells on a grid. A specified volume of cells was mixed with a solution of the complex in various concentrations. The solutions of the complexes were prepared by making a stock solution of each and through dilution the desired concentrations were obtained. The concentrations ranged from 0.01μM titanium up to 100μM titanium. The stock solutions were prepared by weighing the complexes in sterile tubes and then dissolving them in DMSO, where after the solution was diluted with an aqueous NaCl solution. The ratio was kept at 1:9 DMSO:NaCl(aq). The cells were incubated for three days at body temperature and afterwards the cells were dyed and the intensity of the color was measured. The color intensity was directly proportional to the number of living cells. It was then possible to plot the results and make comparisons. Each experiment was done in triplicate and the average value was recorded as shown in Appendix **D**. The results were graphically presented and discussed in Section 5.2.

6.6 Studies related to the antitumor activities of the complexes

Intercalation studies

The intercalation tests were done in triplicate by an application of a technique derived from flow cytometry and results were expressed as an average of three experiments. A human cervix epithelial cell line (HeLa:ATCC CC42) was grown as monolayer cultures using Minimum Essential Medium (MEM) supplemented with 10% fetal calf serum (FCS). For the flow cytometry assays , cells were made up in Hepes buffer (HBSS-Hepes buffer) containing 0.4mg/ml propidium iodide. Each sample was treated with a different concentration (0.03 - 0.01μg/ml) of the intercalator or metal complex. To measure the damage to the DNA a nucleoid sedimentation technique using a flow cytometer (Coulter XL-MCL)-based laser light scattering system was used[10]. The measurement was done after a 30 minute treatment at 4°C, with the exeption of H_2O_2 (incubated for 15 minutes at 37°C). The median for the forward and side scatter was calculated for each concentration and was reported as the median channel number. The results are tabulated in Appendix **E** and discussed in Section 5.5.

Ligand substitution in aqueous medium

The displacement of ligands from the coordination sphere of the titanium in aqueous solution was studied with NMR. During this experiment, titanocene dichloride and the mono and bis substituted

10. A. E. Milner, A. T. M. Vaughan, I. P. Clark, *Radiation Research*, **1987**, *110*, 108.

thiolates derivatives were compared. A titanium compound concentration of 0.25M was prepared for each complex in a mixture of DMSO and 32% saline D_2O in a 1:4 ratio. The samples were kept in a water bath at 37 °C. Samples were run for 64 scans on a Bruker AC-300 spectrometer and over eight time intervals: 0h, 1h, 2h, 4h, 6h, 10h, 20h, 30h and 60h. The data is shown in Appendix **F** and discussed in Section 5.4.

6.7 Crystal structure determinations

Complex 2-05

The X-ray intensity data set for complex 2-05 was collected on a novel 1K SMART Siemens CCD area detector system using Mo radiation[11]. X-rays were generated using a regular sealed tube and an X-ray generator operating at 50kV 30mA. The 9cm wide CCD area detector was mounted 4.5cm from the crystal and the data set collected at low temperature (-100°C). A graphite monochromator followed by a 5mm collimator was used. The selected crystal was mounted on a thin glass fibre.

In order to obtain an initial set of cell parameters and an orientation matrix for data collection, reflections from three sets of 15 frames each were collected, covering three perpendicular sectors of space. The data collection nominally covered over a hemisphere of reciprocal space, by a combination of 3 sets of exposures of 1271 frames. Each set had a different φ angle for the crystal and each exposure covered 0.3° in ω, with 10 seconds exposure per frame. In order to monitor crystal and instrument stability and to enable crystal decay corrections, the first 50 frames of the first set were measured again at the end of the data collection. Crystal decay was found to be negligible after analysing the duplicate reflections. The final data set after scaling consisted of 16945 reflections to 0.751A resolution. Coverage of data is 67.87 % complete to at least 28.26° in θ. The data collection took about 5 hours. A detailed presentation of the data collection statistics is given in Table 6.3

H atoms were placed geometrically and refined with a riding model and with U_{iso} constrained to be $0.08A^2$. Refinement on F^2 for ALL reflections, except for 0 with a very negative F^2 or flagged by the user for potential systematic errors. Weighted R- factors (wR) and all goodness-of-fit (S) are based on F^2, while conventional R-factors (R) are based on F, with F set to zero for negative F^2. The observed criterion of $F^2 > 2\sigma(F^2)$ is used only for calculating R-factor observed, etc. and is not relevant to the choice of reflections for refinement. R-factors based on F^2 are statistically about twice as large as those based on F, and R-factors based on ALL data will be even larger.

11. G. M. Sheldrick, *SADABS User Guide*, University of Göttingen, Germany, **1996**.

All esd's, except the esd in the dihedral angle between two l. s. planes, were estimated using the full covariance matrix. The cell esds were taken into account individually in the estimation of esd's in distances, angles and torsion angles; correlations between esds in cell parameters were only used when they were defined by crystal symmetry. An approximate (isotropic) treatment of cell esds was used for estimating esds involving l. s. planes.

The determination of the unit cell parameters, crystal orientation and data collection were performed with the SMART package (Siemens 1995)[12]. The crystallographic raw data frames were integrated, all reflections extracted, reduced and Lp-corrected using the program SAINT (Siemens 1995)[13]. The cell refinement using all data was also performed by SAINT (Siemens 1995). The program SHELXTL version 5.0 (Siemens 1995) was used for the structure solution, refinement, molecular graphics and publication preparation[14]. The crystal data and structure refinement for **2-05** is shown in Table 6.3. In Appendix **A** the complete tables of the fractional atomic coordinates and equivalent isotropic displacement parameters, bond lengths, bond angles, anisotropic displacement parameters, hydrogen coordinates and isotropic displacement parameters of complex **2-05** are listed.

Complexes 2-02 and 3-09

The intensity data for the compounds were collected on a Nonius KappaCCD diffractometer, using graphite-monochromated Mo-K_α radiation. Data were corrected for Lorentz and polarization effects, but not for absorption effects [15,16]. The structures were solved by direct methods (SHELXS [17]) and refined by full-matrix least squares techniques against Fo^2 (SHELXL-97 [18]). The hydrogen atoms were included at calculated positions with fixed thermal parameters. All nonhydrogen atoms were refined anisotropically[18]. XP (SIEMENS Analytical X-ray Instruments, Inc.) was used for structure representations. The crystal data and structure refinement for **2-02** and **3-09** is shown in Table 6.4 and

12. *Siemens (1996) SMART Reference Manual*, Siemens Analytical X-ray Instruments Inc., Madison, Wisconsin, USA, **1996**.

13. *Siemens (1995b) ASTRO and SAINT. Data Collection and Processing for the SMART System*, Siemens Analytical X-ray Instruments Inc., Madison, Wisconsin, USA, **1995**.

14. *Siemens (1995a) SHELXTL Version 5.0 (Dos version) - Structure Determination Programme*, Siemens Analytical X-ray Instruments Inc., Madison, Wisconsin, USA, **1995**.

15. *COLLECT, Data Collection Software*; Nonius B.V., Netherlands, **1998**.

16. Z. Otwinowski, W. Minor, *„Processing of X-Ray Diffraction Data Collected in Oscillation Mode", in Methods in Enzymology, Macromolecular Crystallography, Part A*, C.W. Carter & R.M. Sweet (eds), Academic Press, **1997**, *276*, 307-326.

17. G. M. Sheldrick, *Acta Crystallogr. Sect. A* , **1990**, *46*, 467-473.

18. G. M. Sheldrick, SHELXL-97 (Release 97-2), University of Göttingen, Germany, **1997**.

Table 6.3. Crystal data and structure refinement for **2-05**.

Empirical formula	$C_{33}H_{41}ClO_3Ti$	
Molecular weight	569.01	
Temperature, K	296(2)	
Wavelength, Å	0.71073	
Space group	P2(1)/n	
Unit cell dimensions:	a = 10.0318(5)Å b = 17.6700(10)Å c = 15.3214(8)Å	α = 90° β = 103.728(1)° γ = 90°
Z	4	
Volume, $Å^3$	2638.3(2)	
Density (calculated), Mg/m^3	1.433	
Absorption coefficient, mm^{-1}	0.461	
F(000)	1208	
Crystal size, mm	0.28 x 0.36 x 0.44	
Scan range (θ°)	$1.79 \leq \theta \leq 28.26$	
Zone collected	$-12 \leq h \leq 9$; $-22 \leq k \leq 21$; $-19 \leq l \leq 20$	
Reflections collected	16714	
Independent reflections	6010	
R_{int}	0.0209	
Data / restraints / parameters	6010 / 0 / 411	
Goodness-of-fit on F^2	1.840	
Final R indices [$I>2\sigma(I)$]	R1 = 0.0610; wR2 = 0.2122	
R indices (all data)	R1 = 0.0674; wR2 = 0.2187	
Residual electron density, ($eÅ^{-3}$)	Max = 1.564; Min = -0.710	

Table 6.5 respectively. In Appendix **B** and Appendix **C** the complete tables of the fractional atomic coordinates and equivalent isotropic displacement parameters, bond lengths, bond angles, anisotropic displacement parameters, hydrogen coordinates and isotropic displacement parameters of complexes **2-02** and **3-09** are listed respectively.

Table 6.4. Crystal data and structure refinement for **2-02**.

Identification code	FO1047	
Empirical formula	$C_{34}H_{24}O_2Ti$	
Formula weight	512.43	
Temperature	183(2) K	
Wavelength	0.71073 Å	
Crystal system	Monoclinic	
Space group	P2(1)/c	
Unit cell dimensions	a = 12.4323(6) Å b = 12.6852(7) Å c = 31.796(1) Å	a = 12.4323(6) Å b = 12.6852(7) Å c = 31.796(1) Å
Volume	4988.6(4) $Å^3$	
Z	8	
Density (calculated)	1.365 g/cm^3	
Absorption coefficient	0.374 mm^{-1}	
F(000)	2128	
Crystal size	0.28 x 0.22 x 0.10 mm^3	
Theta range for data collection	3.11 to 30.99°.	
Index ranges	-17<=h<=17, -7<=k<=18, -44<=l<=44	
Reflections collected	19160	
Independent reflections	13869 [R(int) = 0.1240]	
Completeness to theta = 27.48°	87.4 %	
Absorption correction	0.9636 and 0.9026	
Max. and min. transmission	Full-matrix least-squares on F^2	
Refinement method	13869 / 0 / 667	
Data / restraints / parameters	0.987	
Goodness-of-fit on F^2	R1 = 0.1099, wR2 = 0.1448	
Final R indices [I>2sigma(I)]	R1 = 0.2918, wR2 = 0.1941	
R indices (all data)	0.303 and -0.370 $e.Å^{-3}$	
Largest diff. peak and hole	2128	

Table 6.5. Crystal data and structure refinement for **3-09**.

Identification code	fo1042	
Empirical formula	$C_{22}H_{17}ClS_2Ti$	
Formula weight	428.83	
Temperature	183(2) K	
Wavelength	0.71073 Å	
Crystal system	Monoclinic	
Space group	P2(1)/c	
Unit cell dimensions	a = 11.1309(5) Å b = 7.8238(3) Å c = 21.946(1) Å	α= 90°. β= 96.464(2)°. γ = 90°.
Volume	1899.0(1) $Å^3$	
Z	4	
Density (calculated)	1.500 g/cm^3	
Absorption coefficient	0.814 mm^{-1}	
F(000)	880	
Crystal size	0.28 x 0.22 x 0.18 mm^3	
Theta range for data collection	3.19 to 27.48°.	
Index ranges	-14<=h<=14,-9<=k<=10, -28<=l<=28	
Reflections collected	7637	
Independent reflections	4277 [R(int) = 0.0424]	
Completeness to theta = 27.48°	98.2 %	
Absorption correction	None	
Max. and min. transmission	0.8673 and 0.8041	
Refinement method	Full-matrix least-squares on F^2	
Data / restraints / parameters	4277 / 0 / 235	
Goodness-of-fit on F^2	1.022	
Final R indices [I>2sigma(I)]	R1 = 0.0424, wR2 = 0.0877	
R indices (all data)	R1 = 0.0705, wR2 = 0.0967	
Largest diff. peak and hole	0.267 and -0.469 $e.Å^{-3}$	